Journal of
Water & Climate Change



IWA PUBLISHING



Journal of Water and Climate Change Vol 15 No 2, 628 doi: 10.2166/wcc.2023.521

# Climate change-induced drought and implications on maize cultivation area in the upper Nan River Basin, Thailand

Rabin Bastola[a,b], Sangam Shrestha[a,*], S. Mohanasundaram[a] and Ho Huu Loc[a]

[a] Water Engineering and Management, Department of Civil and Infrastructure Engineering, School of Engineering and Technology, Asian Institute of Technology, Pathum Thani 12120, Thailand
[b] Department of Environmental Science, Amrit Campus, Tribhuvan University, Kathmandu, Nepal
*Corresponding author. E-mail: sangam@ait.asia

SS, 0000-0002-4972-3969

## ABSTRACT

The escalating frequency of climate change-induced droughts poses a severe threat to rainfed maize cultivation in Thailand's upper Nan River Basin (NRB). Utilizing the standardized precipitation evapotranspiration index, this study comprehensively examines spatial and temporal drought patterns and their potential agricultural impact. Findings indicate a significant shift in precipitation patterns with wetter wet seasons, drier dry seasons and rising temperatures. The upper NRB experiences prolonged and severe droughts, while the lower region faces higher drought intensity, signalling an increased likelihood of extended and severe drought episodes in the upper region. Assessing maize cultivation suitability, factoring in environmental variables and drought impact under observed and climate change scenarios, reveals the current moderate suitability at 42.2%, projected to expand, and unsuitable regions expected to double. Different shared socioeconomic pathways (SSPs) show varied outcomes, with SSP5-8.5 indicating increased suitability in highly suitable areas and SSP2-4.5 demonstrating improvements in moderately suitable areas. The study underscores the need for tailored adaptation strategies in water management during droughts to enhance crop production, especially in dry seasons, in the upper NRB amid a changing climate.

**Key words:** CMIP6, drought, maize suitability area, Nan River Basin, SPEI

## HIGHLIGHTS

- The upper Nan River Basin (NRB) tends to experience a wetter wet season and drier dry season with rising temperatures.
- The upper region of the basin will likely experience extended periods of drought with higher severity.
- The research findings highlight the impact of drought severity and other environmental variables on maize cultivation in the upper NRB.

## GRAPHICAL ABSTRACT

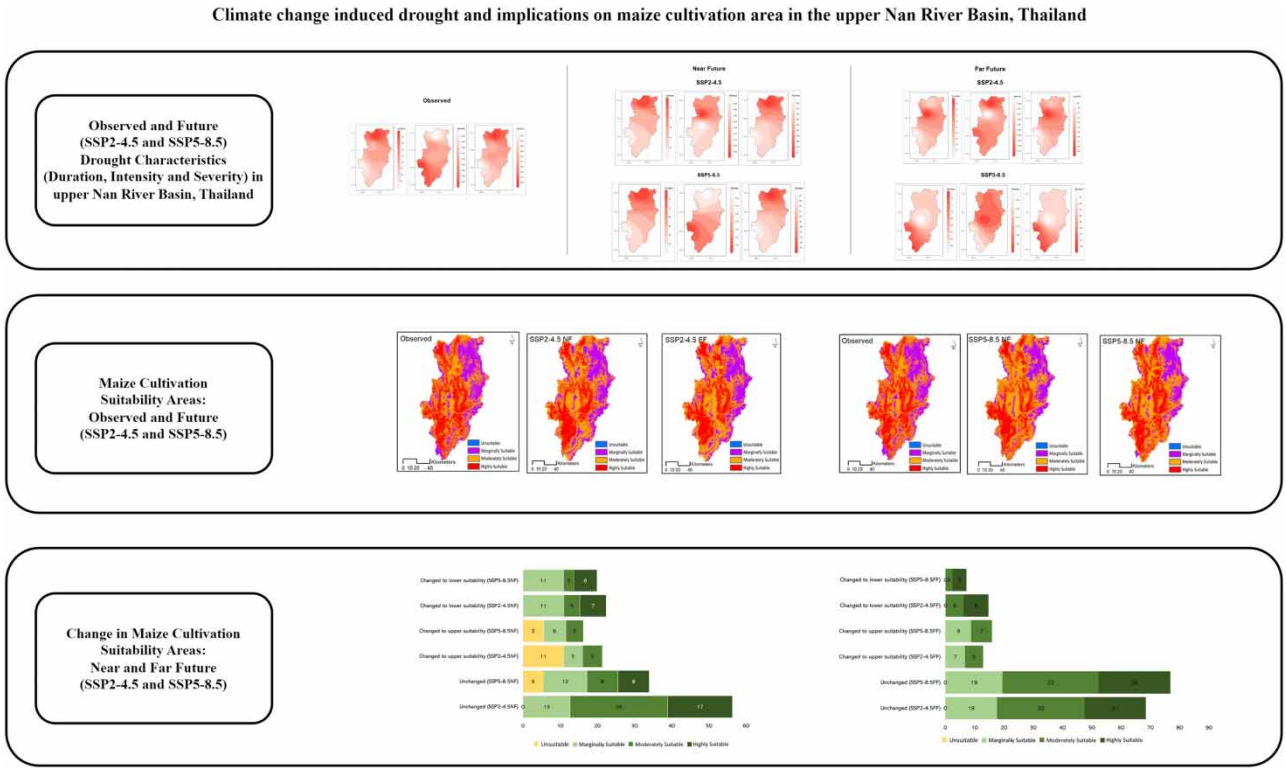


## 1. INTRODUCTION

Drought is one of the major consequences of climate change, with prolonged droughts posing a major challenge to agricultural production due to their extended duration (Ahmadalipour *et al.* 2017; Peña-Gallardo *et al.* 2019). The spatial and temporal distribution of drought has significant impacts on availability of water and other environmental attributes, altering bioclimatic envelope of many plants, including those of agriculture significance (Dai *et al.* 2020; Jiang *et al.* 2022; Li *et al.* 2020). The frequency of droughts is on the rise globally, including in the Mekong area of Thailand, leading to increased food insecurity and economic losses (Muangthong *et al.* 2020; Byakatonda *et al.* 2021; Kang *et al.* 2021). Several studies have investigated future drought characteristics in Thailand and shown that northern Thailand, particularly the lower Mekong Basin, may experience more severe and intense droughts (Thilakarathne & Sridhar 2017; Byakatonda *et al.* 2021; Kang *et al.* 2021). However, such studies are very limited in northern Thailand (Arunrat *et al.* 2022), and none of them discuss the potential implications of droughts on maize suitability in the Nan River Basin (NRB).

Drought significantly impacts agricultural productivity through various pathways (Gornall *et al.* 2010; Brown *et al.* 2015). The extent of these impacts depends on the characteristics of drought, such as frequency, intensity and duration, as well as the specific crop varieties being considered (Mishra & Singh 2010). Agriculture plays a pivotal role in Thailand's economy, contributing 8.3% to the gross domestic product in 2016 (Office of Agricultural Economics 2017; Office of The National Economic and Social Development Board 2017). The sector faces significant challenges due to climate change, including rising temperatures and altered rainfall patterns, resulting in reduced crop yields, especially in rural areas where agriculture is the primary occupation (Gentle & Maraseni 2012). In northern Thailand, drought further exacerbates agricultural productivity, particularly in regions heavily dependent on rainfed farming, such as the study site, where prolonged droughts have detrimental effects (Gornall *et al.* 2010; Brown *et al.* 2015; Ahmadalipour *et al.* 2017). Maize, a crucial crop in Northern Thailand, holds the second position after rice, with over 64% of the country's maize cultivation occurring in the Northern region (Grudloyma 2014).

The study emphasizes the need for climate change impact assessments across sectors, including agriculture, in Northern Thailand (Amnuaylojaroen *et al.* 2021). Water availability is crucial for agriculture in this region, where a lack of water

storage infrastructure during non-rainy seasons presents a challenge, and the Nan River's water supply is intricately linked to upstream land use and land cover (Baicha 2016). Moreover, most of the arable (88%) land in the upper NRB is rainfed; therefore, assessing patterns of drought and its impact on agriculture land is essential. To address these concerns, the study focuses on assessing drought risk and its implications on maize-suitable area to guide adaptation planning.

The agricultural sector in Thailand covered 46.5% of the total land area in 2015, and over 34% of the Thai population depends on the agricultural sector for their livelihood (Office of Agricultural Economics 2015). Natural forest area in Nan Province, Thailand, decreased by 41.5% between 1995 and 2012, while the agricultural land area increased by 51.1% (Baicha 2016), increasing demand for agricultural water. Subsequently, local farmers have perceived changes in climatic patterns with a negative impact on farming (Shrestha & Arunyawat 2017).

Understanding the spatial and temporal patterns of drought under different climate change scenarios and their effects on maize cultivation is crucial for devising appropriate strategies to strengthen community resilience in coping with future drought scenarios. Standardized precipitation evapotranspiration index (SPEI) is commonly used to identify and monitor the various levels of drought conditions (Vicente-Serrano *et al.* 2010; World Meterological Organization (WMO) and Global Water Partnership (GWP) 2016). The SPEI accounts for the effect of temperature on drought development, making it a more robust indicator for drought assessment.

In this study, we aim to investigate the patterns of observed and future drought patterns, including spatial and temporal trends, spatial distribution, intensity and duration, using SPEI as the drought indicator. We used recently available CMIP6 datasets, which are commonly used for similar studies (Arunrat *et al.* 2022; Muthuvel *et al.* 2023). The CMIP6 dataset better captures the key elements of future climate conditions compared to other candidate models like CMIP5, providing essential information for drought risk management (Li *et al.* 2020; Ukkola *et al.* 2020; Zhai *et al.* 2020). In addition, we aim to model the maize-suitable areas based on the predicted pattern of drought and examine the potential impact of drought on the maize-suitable areas in the upper NRB, providing critical information for water-related decision-makers and the development of site-specific adaptation strategies.

## 2. DATA AND METHODOLOGY

### 2.1. Study area

The upper NRB is located in the northern part of Thailand, between 99°51′ E to 101°21′ E longitude and 15°42′ N to 18°37′ N latitude (Figure 1). The upper NRB is one of the major sub-basins of the Chao Phraya River Basin, contributing approximately 25–40% of the total flow of the Chao Phraya River, which is a vital water resource for the country (Chuenchum *et al.* 2017). This study, however, will only consider the upper part of the basin, which covers an area of 13,130 $km^2$. The Nan River, which originates in the north of the province and flows southward to the Sirikit Dam, joins with other rivers to form the Chao Phraya River.

The climate of the upper NRB region is significantly influenced by the southwest and northwest monsoons and tropical depressions from the South China Sea, which occur from July to September. The wet season in the region, which occurs between May and October, accounts for about 85% of the annual rainfall, with a bimodal pattern of rainfall distribution, peaking in May and August (Petpongpan *et al.* 2021). The average temperature in the region is approximately 25.6 °C, with an annual precipitation of 1,382 mm (Wangpimool *et al.* 2013). The basin experiences two distinct seasons, namely, the wet season and dry season, where the former spans from May to October, while the latter lasts from November to April. The temperature gradually increases downstream, with temperatures ranging from 8.0 °C at the river source area in Bo Kluea District towards the border with Lao PDR to 20.7 °C near the Sirikit Dam in Uttaradit Province of Thailand.

Approximately 35% of the basin area is used for cultivation. Maize is the primary crop in the basin, occupying more than 10% of the total cultivated area. A recent study on the impact of climate change on crop production in northern Thailand found that the production of rainfed rice and maize may decline by 5 and 4%, respectively (Amnuaylojaroen *et al.* 2021). Moreover, more than 64% of the total maize cultivation area is situated in the northern part of Thailand (Grudloyma 2014). Promising adaptation strategies for improving crop production include additional irrigation, crop diversification and appropriate planting dates, which require further evaluation (Amnuaylojaroen *et al.* 2021).

### 2.2. Future climate projections

Observed meteorological data (1986–2020) were used in this study (Table 1). A total of 16 meteorological stations were used to represent the upper NRB climate from 1981 to 2014.

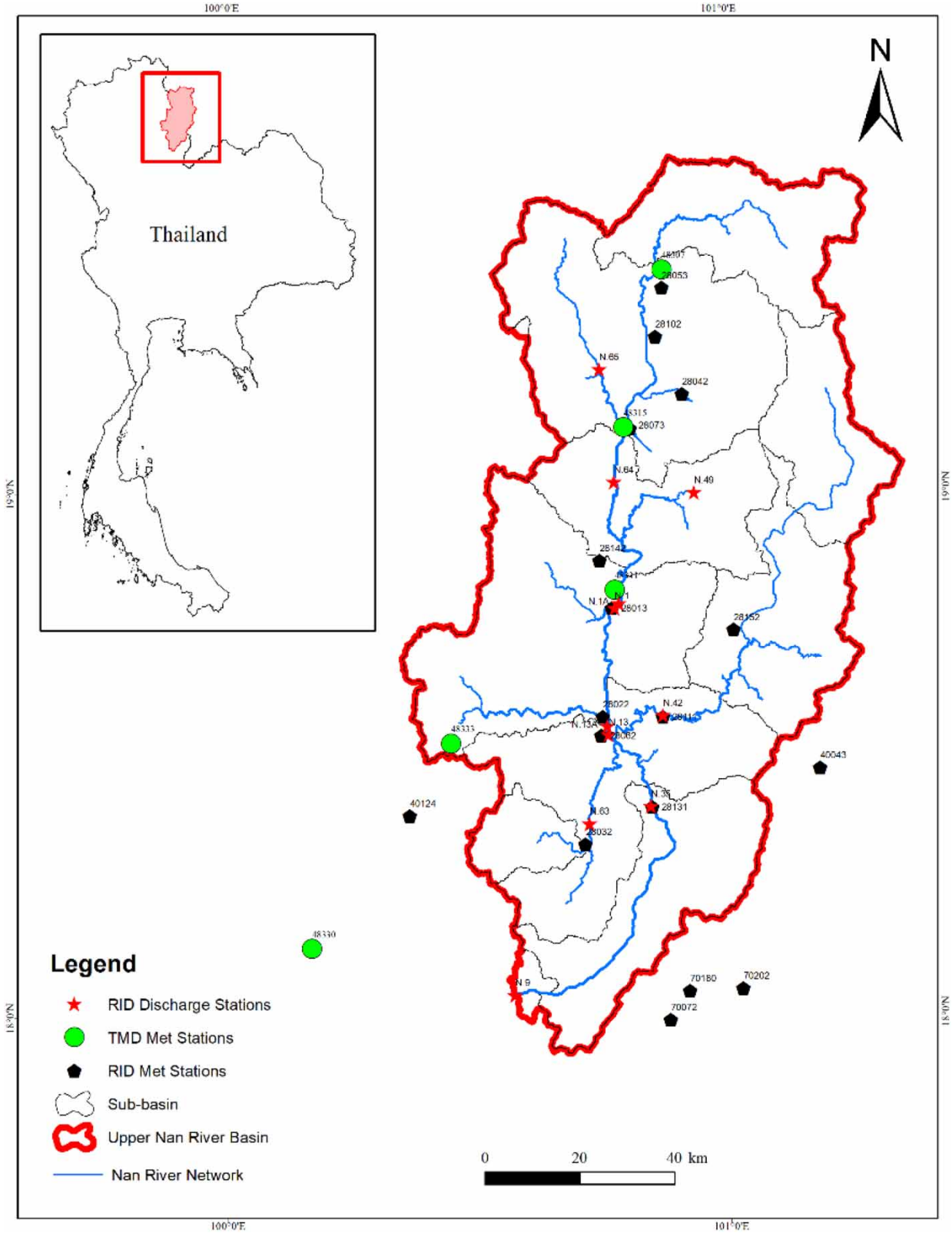


**Figure 1** | Location of upper NRB in Thailand and its hydrological and meteorological stations.

**Table 1** | Geographical information of the meteorological stations in the upper NRB

| SN | Station ID | Location | Latitude | Longitude | Elevation (m above mean sea level) |
|---|---|---|---|---|---|
| 1 | 28022 | Wiang Sa, Nan | 18° 34′ | 100° 45′ | 192 |
| 2 | 28032 | Na Noi, Nan | 18° 19′ | 100° 43′ | 262 |
| 3 | 28042 | Pua, Nan | 19° 10′ | 100° 55′ | 252 |
| 4 | 28073 | Tha Wang Pha, Nan | 19° 07′ | 100° 48′ | 230 |
| 5 | 28102 | Chiang Klang, Nan | 19° 17′ | 100° 51′ | 262 |
| 6 | 28142 | Mueang, Nan | 18° 52′ | 100° 45′ | 302 |
| 7 | 28152 | Mae Charim, Nan | 18° 44′ | 100° 01′ | 431 |
| 8 | 40043 | Song, Phrae | 18° 28′ | 100° 11′ | 162 |
| 9 | 40124 | Rong Kwang, Phrae | 18° 23′ | 100° 22′ | 205 |
| 10 | 70072 | Fak Tha, Uttaradit | 17° 59′ | 100° 52′ | 265 |
| 11 | 70202 | Ban Khok, Uttaradit | 18° 02′ | 100° 01′ | 385 |
| 12 | 48307 | Thung Chang, Nan | 19° 25′ | 100° 52′ | 333 |
| 13 | 48315 | Tha Wangpha, Nan | 19° 07′ | 100° 47′ | 235 |
| 14 | 48330 | Phrae | 18° 07′ | 100° 10′ | 162 |
| 15 | 48331 | Nan | 18° 48′ | 100° 46′ | 200 |
| 16 | 48333 | Agromet, Nan | 18° 31′ | 100° 27′ | 610 |

The CMIP6 models have been used in this study. The CMIP6 model simulations have enhanced the performance of temperature and regional rainfall projections (Eyring *et al.* 2019; Zhu & Yang 2020). In this study, two scenarios, i.e., SSP2-RCP4.5 (SSP2-4.5) and SSP5-RCP8.5 (SSP5-8.5), are considered (Riahi *et al.* 2011). Four CMIP6 global climate models (GCM) (CMCC-ESM2, EC-Earth3, EC-Earth3-CC and GFDL-ESM4) were selected for this study to project future climate (2023–2097) (Table 2).

The climatic variables include daily maximum near-surface air temperature (*tasmax*), daily minimum near-surface air temperature (*tasmin*) and precipitation (*pr*). These GCMs have been widely used in similar studies (Cook *et al.* 2020; Ukkola *et al.* 2020; Iqbal *et al.* 2021; Schwarzwald *et al.* 2021; Yue *et al.* 2021). The entire study period was divided into three 35-year periods for equal comparison, i.e., history (from 1986 to 2020), near future (NF; from 2023 to 2057) and far future (FF; from 2063 to 2097).

### 2.3. Bias correction of climate data

The quantile mapping technique was used to bias correct the GCMs with the observation data provided by the Royal Irrigation Department (RID) and Thai Meteorological Department (TMD). This is a non-parametric bias correction method (Shrestha *et al.* 2017; Yue *et al.* 2021). Quantile mapping is based on daily constructed empirical cumulative distribution functions (ECDFs) and can improve the median, variance, frequency, intensity and extremes (Themeßl *et al.* 2012). The

**Table 2** | Information about CMIP GCMs used in this study

| Model | Institution/Country | Reference |
|---|---|---|
| CMCC-ESM2 | The Centro Euro-Mediterraneo sui Cambiamenti Climatici, Italy | Iqbal *et al.* (2021); Lovato *et al.* (2022) |
| EC-Earth3 | EC-Earth Consortium, Europe | Massonnet *et al.* (2020); Khadka *et al.* (2021); Döscher *et al.* (2021) |
| EC-Earth3-CC | EC-Earth Consortium, Europe | Swart *et al.* (2019); Zhu & Yang (2020); Khadka *et al.* (2021); |
| GFDL-ESM4 | Geophysical Fluid Dynamics Laboratory (GFDL), USA | Dunne *et al.* (2020); Supharatid *et al.* (2021) |

method corrects the distribution shape of the daily precipitation based on daily constructed pointwise ECDFs. Both wet and dry days are included in the ECDF estimation. Thus, the frequency of precipitation occurrence is corrected along with its quantity. The temperature is corrected on the basis of theoretical distribution.

$$Y_{t,i}^{\mathrm{cor}} = X_{t,i}^{\mathrm{raw}} + \mathrm{CF}_{t,i} \tag{1}$$

$$\mathrm{CF}_{t,i} = \mathrm{ecdf}_{\mathrm{doy},i}^{\mathrm{obs,cal}^{-1}}(P_{t,i}) - \mathrm{ecdf}_{\mathrm{doy},i}^{\mathrm{mod,cal}^{-1}}(P_{t,i}) \tag{2}$$

$$P_{t,i} = \mathrm{ecdf}_{\mathrm{doy},i}^{\mathrm{obs,cal}} X_{t,i}^{\mathrm{raw}} \tag{3}$$

where CF is the difference between the observed and modelled inverse ecdf for the respective day of the year in the calibration period at probability $P$, ecdf is the empirical cumulative density distribution, ecdf-1 is the inverse empirical cumulative density distribution, $t$ represents daily, $i$ is the grid cell, obs is the observed data, mod is the model data, doy is the day of the year, cal is the calibration period and $X^{\mathrm{raw}}$ is the raw climate model output.

Four GCMs were corrected based on observed climate data obtained from the RID and TMD. Data from five stations were used for correcting the maximum and minimum temperatures and 11 rain gauge stations for correcting the rainfall. The bias correction performance was evaluated using the mean, standard deviation, root mean square error and coefficient of determination ($R^2$). An ensemble of four GCMs was used to represent the climate in the basin under future climate scenarios.

### 2.4. Calculation of standardized precipitation evapotranspiration index

Different indices assess drought, but subjectivity in its definition makes a unique and universal index challenging to establish (Heim 2002). The SPEI gains consensus as a common drought index because it considers both rainfall and temperature (Vicente-Serrano *et al.* 2010).

Drought metrics include duration ($D$), intensity ($I$) and severity ($S$). Duration refers to consecutive months below the drought threshold, while frequency is the number of drought events over time (Figure 2). Intensity is the difference between the threshold and the monthly running mean drought index during a drought. Severity is the cumulative intensity over the drought period (Ukkola *et al.* 2020).

SPEI is used in this study for meteorological drought analysis. It uses the concept of 'climatic water balance,' which considers the difference between precipitation and potential evapotranspiration (PET) (Peña-Gallardo *et al.* 2019). PET is calculated using the Hargreaves method (Hargreaves & Samani 1985), providing an alternative to the Penman–Monteith method.

Standardized precipitation index/SPEI calculation timescales range from 1 to 48 months or longer, denoted as SPI1 (SPEI1), SPI2 (SPEI2) and so on (World Meteorological Organization 2012). For annual drought trend and intensity,

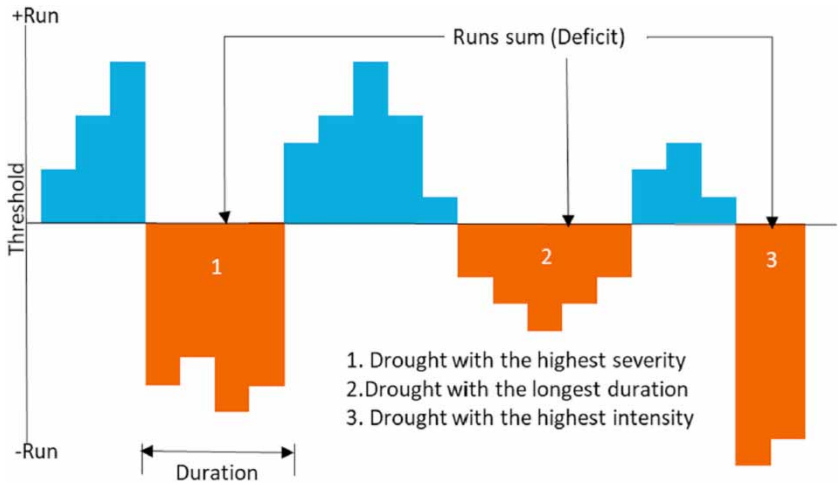


**Figure 2** | Schematic diagram of run theory showing variables of drought – duration, intensity and severity (Lee *et al.* 2017).

SPEI12 in December is used (Sections 3.1 and 3.3). SPEI6 in May and November represent the dry and wet seasons, respectively, based on data from the past 6 months. SPEI3 is used in Section 3.2, as it reflects drought characteristics and the widespread impact of seasonal drought in tropical and temperate regions, particularly in primary agricultural regions (WMO 2012; Ukkola *et al.* 2020).

In this study, the SPEI values are calculated for 3-, 6- and 12-month timescales for each meteorological station. Calculations were performed using the 'SPEI package' available in R-program (Vicente-Serrano *et al.* 2010). The calculation of the SPEI is briefly described as follows:

(a) Calculate the difference between precipitation and PET on the monthly basis (Equation (4)):

$$D_j = P_j - \mathrm{PET}_j \tag{4}$$

The PET was calculated using the Hargreaves equation as it performs relatively close to the standard Food and Agricultural Organization equation (Allen *et al.* 1998).

(b) The next step is to calculate the accumulated difference between precipitation and PET at different timescales. The accumulated difference ($X_{i,j}^k$) at the $k$-month timescale is calculated using Equation (5):

$$\begin{aligned} X_{i,j}^k &= \sum_{l=13-k+j}^{12} D_{i-1,\,l} + \sum_{l=1}^{j} D_{i,\,j} \quad \text{if} \quad j < k \\ X_{i,j}^k &= \sum_{i=j-k+1}^{j} D_{i,\,j} \qquad\qquad \text{if } j \geq k \end{aligned} \tag{5}$$

where $X_{i,j}^k$ is the accumulated difference between precipitation and the PET at the $k$-month timescale in the $j$th month of the $i$th year; $D_{i,l}$ is the monthly difference between the precipitation and the PET in the $l$ month of the $i$th year.

(c) Normalize the $X_{i,j}^k$ data sequence. Because there may be negative values in the original data sequence $X_{i,j}^k$, therefore, the SPEI uses the three-parameter log-logistic probability distribution (Vicente-Serrano *et al.* 2010). For the data sequence of all timescales, the accumulative function of the log-logistic probability distribution $F(X)$ is given in Equation (6):

$$F(X) = \left[1 + \left(\frac{\alpha}{x - \gamma}\right)^{\beta}\right]^{-1} \tag{6}$$

where $\alpha$, $\beta$ and $\gamma$ are scale, shape and position parameters, respectively, which can be calculated using the equations proposed by Vicente-Serrano *et al.* (2010).

$p$ is the probability of a definite $X_{i,j}^k$ value:

$$p = 1 - F(X) \tag{7}$$

If $p \leq 0.5$,

$$w = \sqrt{-2\ln p} \tag{8}$$

$$\mathrm{SPEI} = w - \frac{C_0 + C_1 w + C_2 w^2}{1 + d_1 w + d_2 w^2 + d_3 w^3} \tag{9}$$

If $p > 0.5$,

$$w = \sqrt{-2\ln(1-p)} \tag{10}$$

$$\text{SPEI} = \frac{C_0 + C_1 w + C_2 w^2}{1 + d_1 w + d_2 w^2 + d_3 w^3} \tag{11}$$

where $C_0 = 2.515517$, $C_1 = 0.802853$, $C_2 = 0.010328$ $d_1 = 1.432788$, $d_2 = 0.189269$ and $d_3 = 0.001308$.

The calculated values of the SPEI are classified as shown in Table 3 and are used to analyse the characteristics of dry and wet events in the basin in terms of their duration, severity and intensity of dry and wet events. The duration of an event is the length of time (months) that the SPEI is consecutively at or below a truncation level. The drought duration ($D$) is the period length in which the SPEI is continuously negative, starting from the SPEI values equal to $-1$ and ending when the SPEI values turn out to be positive. The drought severity ($S$) is the cumulated SPEI values within the drought duration, which is defined by:

$$\text{Severity } (S) = -\sum_{i=1}^{D} \text{SPEI}_i \tag{12}$$

and intensity of drought is the ratio of severity of drought to its duration. Events that have shorter duration and higher severities will have large intensities.

$$\text{Intensity } (I) = \frac{S}{D} \tag{13}$$

### 2.5. Mann–Kendall's trend and Sen's slope estimation

The Mann–Kendall (MK) test is a non-dimensional statistical method used to detect trends in time series (Mann 1945; Kendall 1975), and is recommend by the World Meteorological Organization (WMO) for trend analysis (Liu *et al.* 2020). The MK test was employed to examine the temporal trend of SPEI in this study. For all results, the significance of the trend was tested at the 5% level.

Sen's slope estimation is a non-parametric method (Sen 1968) used to determine the magnitude of the trend in hydrometeorological data. The method involves computing slopes for all the pairs of ordinal time points and then using the median of these slopes as the estimate of the overall slope. This method is not affected by outliers in data and can effectively quantify the trend in a time series data. The estimate of the trend slope $Q$ is given by:

$$Q = \text{Median}\left[\frac{x_j - x_k}{j-k}\right] \; k < j \tag{14}$$

where for $i = 1, 2, \ldots, N$, $x_j$ is the data value at time $j$, $x_k$ is the data value at time $k$ and $j$ is the time after $k$ ($j > k$) and $N$ is a number of all pairs $x_j$ and $x_k$.

### 2.6. Inverse distance weighting interpolation

To analyse the spatial patterns of the magnitudes and trends of SPEI, the inverse distance weighting algorithm (Fluixá-Sanmartín *et al.* 2016) was used, which is widely applied to map the spatial extent of climatic and hydrological point data (Feng *et al.* 2017; Ma *et al.* 2017). The method is a deterministic interpolation assuming that the sample values closer to

**Table 3** | Classification of the severity of dry and wet events based on the calculated SPEI

| Category | SPEI value |
|---|---|
| Extreme dryness | Less than −2 |
| Severe dryness | −1.99 to −1.5 |
| Moderate dryness | −1.49 to −1.0 |

the prediction location are more representative than sample values farther away (Ashraf & Routray 2015). Thus, the closest value to the prediction location receives the maximum weight, and the weight is decreased as a function of distance (Liu *et al.* 2020).

### 2.7. Modelling impact of drought on suitability of maize cultivation area

We prepared maize suitability maps using both physical and bioclimatic variables. We used the maximum entropy model (Phillips *et al.* 2006), known as MaxEnt, which is based upon ecological niche theory, that predicts the distribution of a species over an area from environmental data and species occurrence records (Guisan & Zimmermann 2000). The MaxEnt model works with 'presence-only data' and has outperformed other presence-only modelling algorithms (e.g., Hernandez *et al.* 2006; Aguirre-Gutiérrez *et al.* 2013). It is a widely used tool to evaluate the suitability of areas and its spatial distribution for a particular species.

#### 2.7.1. Maize presence data

We derived the maize presence locations from the land use and land cover map of Nan Province. The map includes 'maize cultivation' area as one of the categories. We generated 500 random points from the maize cultivation area with a linear distance at least of 500 m to avoid spatial autocorrelation in the model.

#### 2.7.2. Environment variables

Environmental variables include those that potentially influence suitability of maize cultivation (Fu *et al.* 2011; He & Zhou 2012; Tashayo *et al.* 2020). We selected physical variables, namely, elevation, slope, aspects, soil and profile curvature, as environmental variables to predict areas suitable for maize cultivation as these variables have a major influence of maize cultivation. Changes in elevation significantly impact various environmental factors, including soil water content, precipitation, radiation and temperature. These elements fluctuate based on the elevation above the sea level, influencing maize yield, growth and distribution (Tashayo *et al.* 2020). Slope also affects maize suitability through various pathways. Generally, low slope land is more suitable for maize farming (He & Zhou 2012). The steepness of the slope greatly influences the choice of irrigation methods, drainage rates and mechanization in agricultural activities. Moreover, it indirectly has adverse effects on soil properties and reduces the crop yield (Fu *et al.* 2011; Tashayo *et al.* 2020). Profile curvature is a measure of curvature parallel to slope direction and has direct implication with water flow acceleration. Aspect is an important variable and is the steepest downhill direction. It affects temperature and soil characteristics and moisture. The characteristics of the soil significantly affect the production of maize, and the research findings indicate that the greatest crop output can be achieved with fully irrigated sandy loam soil (Fang & Su 2019).

All these physical variables have an important role in the extent of suitability of maize cultivation (Fu *et al.* 2011; He & Zhou 2012; Tashayo *et al.* 2020). In addition, we used drought characteristics data as a proxy of bioclimatic variable. It includes drought duration, drought severity and intensity, which are derived from minimum and maximum temperature and precipitation. Studies have shown that temperature and precipitation influence maize suitability (He & Zhou 2016; Kogo *et al.* 2019; Neswati *et al.* 2021). Since other bioclimatic variables (e.g., temperature and precipitation) are highly correlated with drought characteristics, we therefore retained drought characteristics only in the models.

#### 2.7.3. Modelling procedure

Maize presence data and selected variables were adapted to the format required for MaxEnt software (v 3.3.3k) (Phillips *et al.* 2006). We selected 75% of maize presence data to build the model, with the remaining 25% used for model verification. We included 10 replicates in our analysis. We used a jackknife estimator to detect the importance of each variable. The model output includes a probability map ranging from 0 to 1. The models were verified by receiver operating characteristic (ROC) curve values, where an ROC value $>0.7$ is considered a good model. We reclassify the map into four suitability classes following criteria of the Intergovernmental Panel on Climate Change as follows: $<0.05$, unsuitable; 0.05–0.33, marginally suitable; 0.33–0.66, moderately suitable; and $>0.66$, highly suitable (Manning 2006; Yue *et al.* 2019). These classes indicate how suitable the respective areas would be for maize cultivation under the given climate change scenarios. This procedure was followed for building maize suitability for mapping of observed drought condition and two climate change pathways (SSP2-4.5 and SSP5-8.5). The ROC values indicated a good performance of the models for all scenarios: observed (0.719), SSP2-4.5 NF (0.722), SSP2-4.5 FF (0.718), SSP5–85.5 NF (0.70) and SSP5–8.5 FF (0.70).

**Table 4** | Mann–Kendall's test results of observed and future SPEI in the upper NRB

| | Observed | | SSP2-4.5 | | SSP5-8.5 | |
|---|---|---|---|---|---|---|
| SPEI | Trend | Slope | Trend | Slope | Trend | Slope |
| Whole year | No trend | −0.0220 | Increasing | 0.0341 | Increasing | 0.0939 |
| Dry season | No trend | −0.0001 | Increasing | 0.0222 | Increasing | 0.0376 |
| Wet season | No trend | −0.0034 | Increasing | 0.0026 | Increasing | 0.0323 |

*Note*: No trend means the trend is not significant ($\alpha = 0.05$).

## 3. RESULTS

### 3.1. Observed and future trend of drought

The observed and future temporal trend of SPEI in the upper NRB is presented in Table 4. The spatial distribution of SPEI in the upper NRB is shown in Figures 3(a)–3(c). The upper NRB will become wetter in the wet season and over the whole year in the future, as demonstrated by SPEI, but the trend is not statistically significant and is also decreasing during the observed period.

There is a rising trend of SPEI in the whole year and wet season in the future period under SSP2-4.5 and SSP5-8.5 (Table 4), but there is no significant and decreasing trend during the observed period for all seasons.

Under SSP2-4.5 and SSP5-8.5, the whole year SPEI (i.e., SPEI12 of December) increased by 0.0341 per year and 0.0939 per year, respectively, across the entire study river basin. The dry season SPEI (i.e., SPEI6 in May) increased by 0.0222 per year and 0.0376 per year, respectively. The wet season SPEI (i.e., SPEI6 of November) increased by 0.0026 per year and 0.0323 per year, respectively.

The whole year, dry season and wet season SPEI of future periods in the upper NRB show slight increases, whereas the observed period SPEI decreased. The results indicate that drought tends to be less severe during wet season and whole year than in the dry season (Figures 3(a)–3(c)). During the last quarter of the 21st century, the wet season will be wetter compared to the earlier future periods. Moreover, the study found that short-term drought events were frequent and alternating throughout the study period, with extreme events in 1992, 2015 and 2019, while long-term droughts lasting more than 6 months occurred, with several before the 1990s and then reappearing after a two-decade gap. The most severe and intense events were observed in 1992 (Table 5).

### 3.2. Spatial distribution of observed and future drought duration, intensity and severity

Observed (1986–2020) and two future periods, i.e., NF (2023–2057) and FF (2063–2097), were compared to analyse changes in future drought duration, intensity and severity in different regions in the upper NRB (Figures 4–6).

Based on the results, the upper region of the basin experienced extended and severe drought, while the intensity of drought was higher in the lower region of the basin during the observed period. The NF under both scenarios show longer drought in the upper region, while the FF under SSP2-4.5 shows longer drought in the mid-region and SSP5-8.5 shows longer drought along the lower stretch of the basin. The severity also follows the same pattern as the duration under NF and FF under both scenarios. However, the intensity of drought during NF and FF under two scenarios shows mixed and contrasting results (Figures 5 and 6).

The NF under SSP2-4.5 and SSP5-8.5 shows longer drought duration in the upper parts of the basin similar to the observed period. The results of SSP5-8.5, however, show shorter drought in most parts of the basin except lower parts during the FF compared to the observed period and future period under SSP2-4.5 scenario. Hence, the upper NRB will experience more wet conditions during FF than in NF.

### 3.3. Temporal evolution and frequency of occurrence of dry and wet events in the basin

We analysed a 35-year observed dataset from 1986 to 2020 and a 75-year projected dataset from 2023 to 2097 under SSP2-4.5 and SSP5-8.5 scenarios to create the 12-month SPEI time series. In Figure 7, we show the evolution of 12-month SPEI values across upper NRB stations, revealing three distinct phases in dry and wet events. From 1986 to 1995, dry events prevailed, while after 2010, drought events increased, often mixed with wet conditions. The future period under SSP2-4.5 and SSP5-8.5

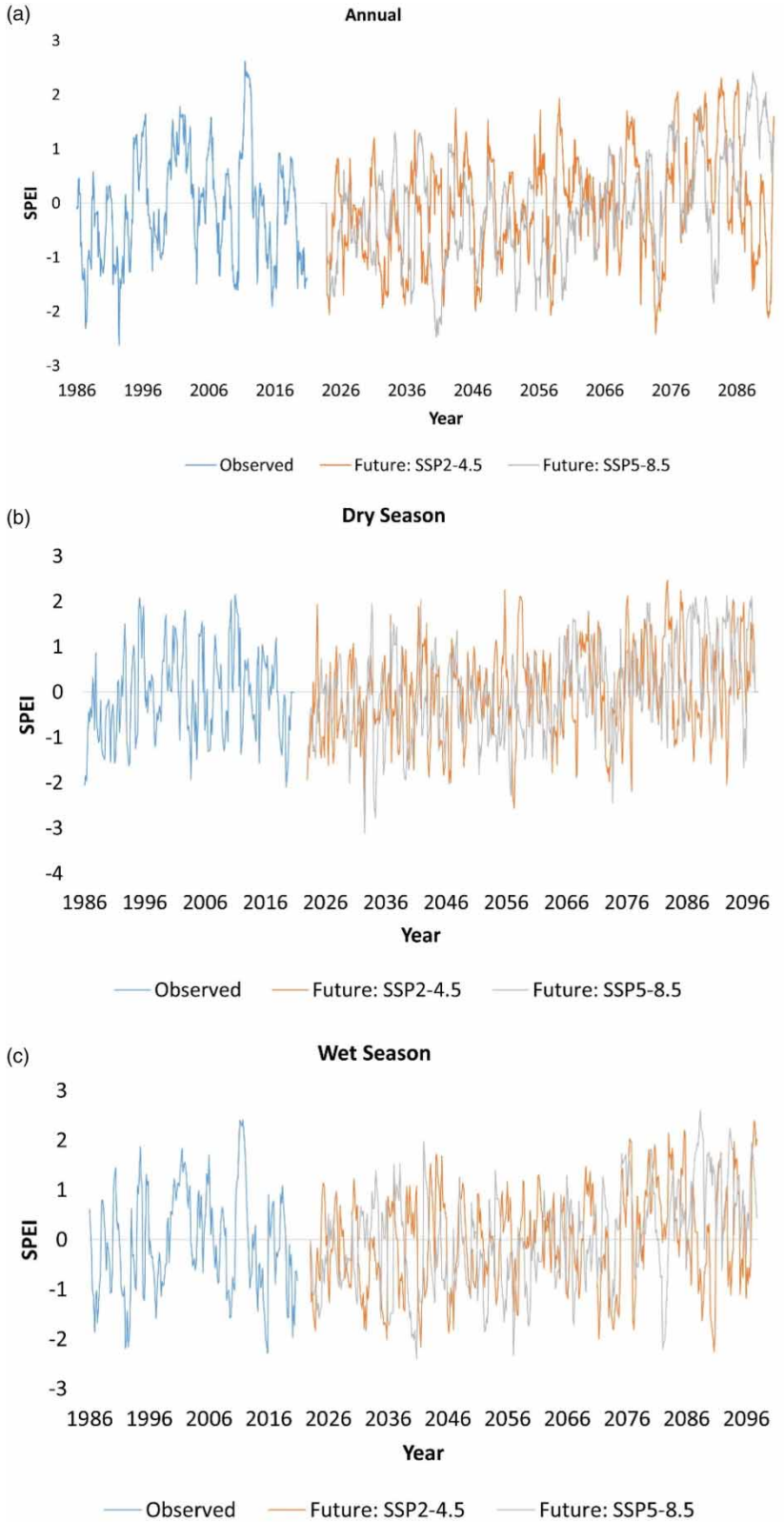


**Figure 3** | Dynamics of observed and future (a) annual, (b) dry season, and (c) wet season SPEI of the upper NRB (future projection is based on average of the four GCM models).

**Table 5** | The duration, severity and intensity of occurrence of some of the major dry events (SPEI $\leq -1$) in the upper NRB during observed period (1986–2020)

| Period of occurrence | Duration | Severity | Intensity |
|---|---|---|---|
| **Dry events for SPEI3** | | | |
| Aug 86–Dec 86 | 4 | −6.69 | −1.67 |
| Aug 89–Oct 89 | 3 | −3.85 | −1.28 |
| Apr 92–Jun 92 | 3 | −5.78 | **−1.93** |
| Nov 93–Feb 94 | 4 | −6.17 | −1.54 |
| Jan 07–Mar 07 | 3 | −4.29 | −1.43 |
| Aug 12–Oct 12 | 3 | −3.99 | −1.33 |
| Jun 15–Aug 15 | 3 | −5.47 | −1.82 |
| Apr 19–Jun 19 | 3 | −4.13 | −1.38 |
| Nov 19–Mar 20 | 5 | −8.58 | −1.72 |
| **Dry events for SPEI6** | | | |
| Aug 86–Jan 87 | 6 | −9.90 | −1.65 |
| May 92–Oct 92 | 6 | −10.86 | **−1.81** |
| Oct 93–Feb 94 | 5 | −6.54 | −1.31 |
| May 09–Jan 10 | 9 | −11.25 | −1.25 |
| Jun 15–Nov 15 | 6 | −10.83 | −1.80 |
| Feb 19–Jul 19 | 6 | −8.15 | −1.36 |
| Feb 20–Jul 20 | 6 | −10.38 | −1.73 |
| **Dry events for SPEI12** | | | |
| Dec 86–Oct 87 | 11 | −17.24 | −1.57 |
| Aug 89–Mar 90 | 8 | −9.46 | −1.18 |
| Jul 91–Jan 92 | 7 | −8.78 | −1.25 |
| Apr 92–Nov 92 | 8 | −13.55 | **−1.69** |
| Aug 09–Jul 10 | 12 | −17.19 | −1.43 |
| Jun 15–Apr 16 | 11 | −16.02 | −1.46 |
| Jul 20–Dec 20 | 6 | −8.48 | −1.41 |

The bold intensity values represent the highest drought intensities at SPEI3, SPEI6, and SPEI12.

shows contrasting pictures. The NF period seems to be dominated by dry events compared to the FF period. Moreover, the FF under SSP5-8.5 scenario shows prolonged wetter condition at the last quarter of the 21st century.

### 3.4. Temporal pattern of observed drought duration, intensity and severity

The temporal pattern of short-term drought (SPEI3) shows that the frequency of alternating dry–wet conditions is higher throughout the study period. The basin experienced extreme short-term drought (SPEI3 $\leq -2$) events in May to June 1992, July 2015, and November 2019. The SPEI6 and SPEI12 represent the long-term water deficiency for almost about a year with considerable fluctuation of the dry and wet events than the SPEI3. A total of seven long-term (more than 6 months) drought events (1986–1987, 1989–1990, 1991–1992, 2009–2010, 2015–2016, and 2020) were observed during the study period. Most of these drought events were frequent before the 1990s and, after a gap of more than two decades, became more frequent, suggesting longer droughts in recent decades over the basin.

The longest duration of dry events for SPEI12 was 12 months (August 2009 to July 2010) followed by 11 months during December 1986 to October 1987 and June 2015 to April 2016). Based on SPEI6, the longest drought event was 9 months, observed during the May 2009 to January 2010 period. Table 5 shows that the most severe dry event for SPEI3, SPEI6 and SPEI12 were observed during November 2019 to March 2020, May 2009 to January 2010, and December 1986 to October 1987 periods, respectively. Moreover, the most intense event was observed during 1992 for all timescales.

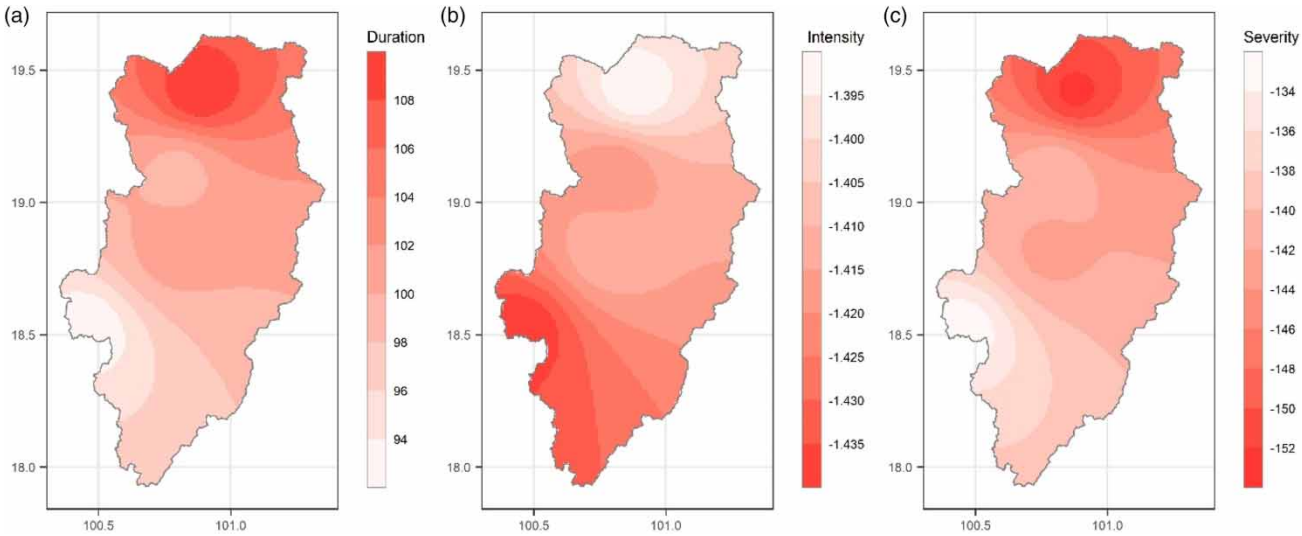


**Figure 4** | Spatial distributions of SPEI3 drought duration (a), unit: month; intensity (b); and severity (c) across the upper NRB for the observed period.

The moderate drought at 3-, 6- and 12-month timescales had the highest frequencies of 8.2, 12.6 and 12.6%, respectively, over the upper NRB (Figure 8). The results also showed that moderate drought frequencies for SPEI3, SPEI6 and SPEI12 were 2.7 (12.0), 3.1 (7.4) and 3.1 (10.6) times higher than the severe and extreme drought frequencies, respectively.

Meanwhile, severe and extreme drought frequencies at the SPEI3 were 3.1 and 0.7%, whereas the severe drought frequency was 2.4 and 3.4 times higher than the extreme drought frequency for 6- and 12-month time timescales.

Overall, the results indicate that the moderate drought was higher than the severe and extreme droughts during the observed period over the upper NRB. The longest short-term drought (SPEI3) was observed in 2019/2020 with a duration of 5 months and a total severity of −8.58. Moreover, the longest duration of 9 and 12 months were observed for SPEI6 and SPEI12, respectively (Table 6).

Moreover, the SPEI6 exhibited the shortest average duration, whereas the SPEI3 demonstrated the lowest average severity (Figure 9). Interestingly, the average intensity remained consistent across all timescales (SPEI3, SPEI6 and SPEI9).

The duration and severity of drought at the SPEI12 and SPEI6 were higher than at the SPEI3, while the intensity was lower in the case of SPEI6 and SPEI12. Further, the increase in duration leads to an enhanced drought severity and intensity at a longer timescale.

### 3.5. Observed and projected seasonal drought distribution

The seasonal distribution of meteorological drought in the future is illustrated in Table 7. Generally, both seasonal droughts are similar during the observed period. Under SSP2-4.5 during the FF period, the percentage of dry season drought under severe and exceptional drought grade is higher (53%) than in wet season (47%). In contrast, under SSP5-8.5 during the FF period, the percentage of wet season drought under severe and exceptional drought grade is higher (54%), while that for dry season is only 46%. The FF results under SSP5-8.5 are like those under SSP2-4.5, with a higher percentage of mild drought higher for dry season and severe and exceptional drought higher for wet seasons.

### 3.6. Impact of drought on maize suitability area

Elevation and slope were among the most important variables describing the distribution of maize cultivation in the upper NRB (Table 8). Other physical factors such as aspect and curvature were not important (Table 8). Among the three characteristics of drought, severity was important in the observed and SSP5-8.5 scenario, whereas intensity was important in SSP2-4.5 scenario.

The areas suitable for maize in the upper NRB, based on observed drought condition, showed that moderately suitable area comprised the highest proportion of the basin (42.2%), followed by highly suitable area (29.2%) and marginally suitable area (28.5%) (Table 9 and Figure 10). Under the SSP2-4.5 NF scenario, there was a slight increase in moderately suitable area

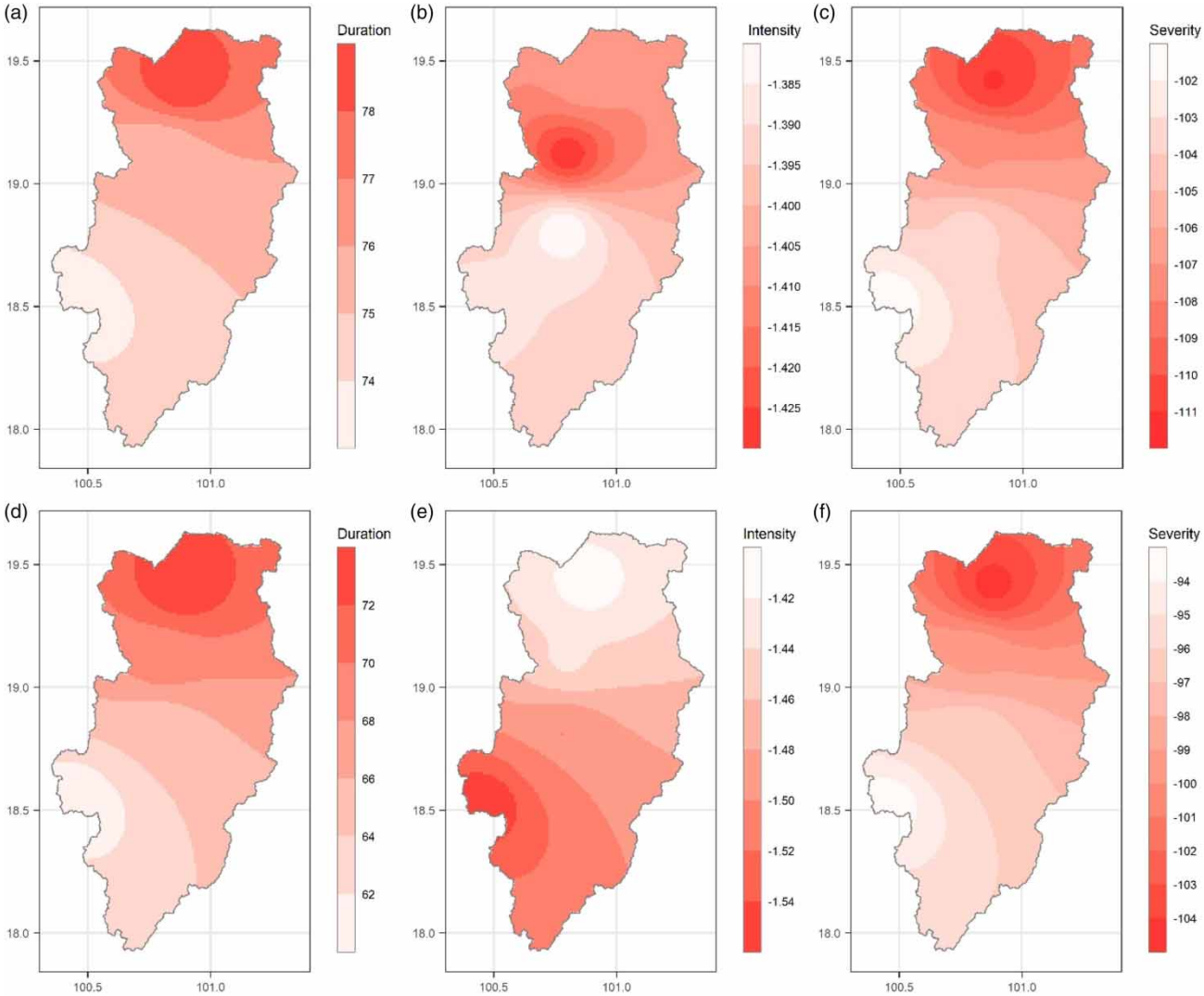


**Figure 5** | Spatial distributions of SPEI3 drought duration (a and d), unit: month; intensity (b and e); and severity (c and f) based on ensemble of CMIP6 GCM models across the upper NRB under SSP2-4.5 and SSP5-8.5 scenarios. The first row figures are for NF (2023–2057) under SSP2-4.5 and second row for NF under SSP5-8.5.

(3.0%), while a decrease in marginally suitable area (1.4%) and highly suitable area (2.4%), and no change in unsuitable area. However, in the case of FF scenario of this projection (SSP2–4.5 FF), the model indicated a double increase in unsuitable area, with a decrease in the marginally suitable area (0.1%), moderately suitable area (0.4%) and highly suitable area (0.2%).

In contrast, there was a double increase in unsuitable area under SSP5-8.5 NF scenario with a decrease in the marginally suitable area (5.5%) and highly suitable area (0.7%). Here, moderately suitable area was projected to increase by 6.2%. Looking further ahead into the FF under SSP5-8.5, a notable increase in highly suitable areas by 3.2% was observed, while marginally suitable areas decreased slightly by 1%. Moreover, unsuitable areas remained the same as observed (0.1%) and moderately suitable areas decrease by 2.2% in comparison with NF projection.

A model showed that the proportions of different land-use classes that remained unchanged, in comparison with the observed one, in the SSP2-4.5 NF and SSP2-4.5 FF scenarios were 56 and 69%, respectively (Figures 11 and 12). Under SSP5-8.5 scenario, the proportion of areas that remained unchanged were 33 and 77% in NF and FF scenarios, respectively.

Thus, in the NF, the unchanged area was high in SSP2-4.5 compared to SSP5-8.5 (Figure 11). There was a reverse pattern in the FF where more area remained unchanged in SSP5-8.5 compared to SSP2-4.5 (Figure 12). Nearly 21% of the area is projected to have improved suitability classes in SSP2-4.5 NF scenarios, which was lower than SSP5-8.5 NF scenario (16%)

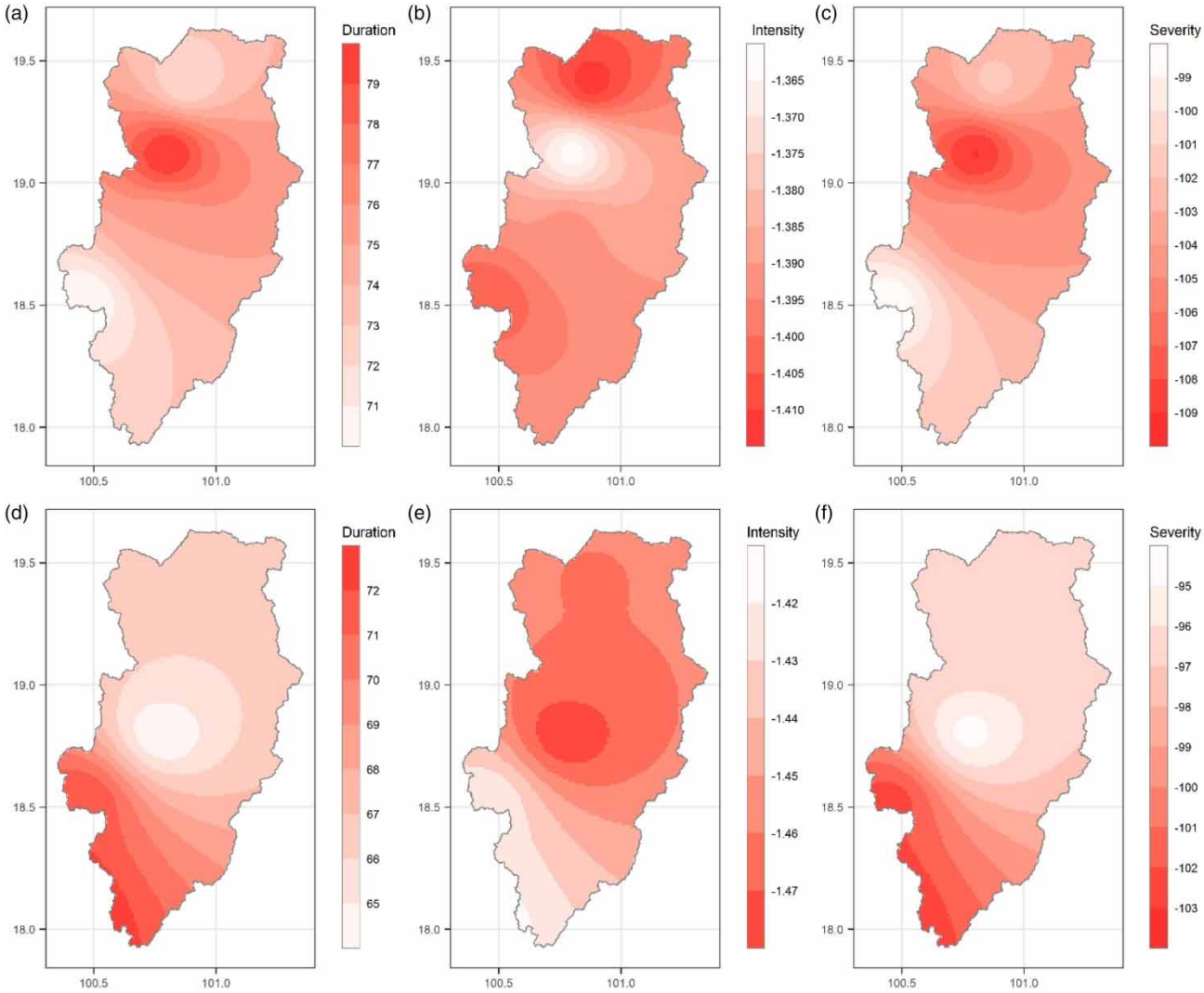


**Figure 6** | Spatial distributions of SPEI3 drought duration (a and d), unit: month; intensity (b and e); and severity (c and f) based on ensemble of CMIP6 GCM models across the upper NRB under SSP2-4.5 and SSP5-8.5 scenarios. The first row figures are for FF (2063–2097) under SSP2-4.5 and second row for FF under SSP5-8.5.

(Figure 11). Here, 22% of the area comprising various categories of maize suitability is projected to have deteriorated suitability classes in SSP2-4.5 NF, the same in SSP5-8.5 NF (20%), suggesting a net deterioration of suitability classes.

Interestingly, nearly 13% of the area is projected to have improved suitability classes in SSP2-4.5 FF scenario, where a slightly higher proportion area (16%) was projected in the SSP5-8.5 FF scenario (Figure 12). Here, 14% of the area comprising various categories of maize suitability is projected to have deteriorated suitability classes in SSP2-4.5 FF, the same in SSP5-8.5 NF (7%), suggesting a net gain of suitability classes (Figure 12).

## 4. DISCUSSION

### 4.1. Evolution of temporal and spatial pattern of drought

The results from this study are overall consistent with previous studies based on the CMIP6 model projections. For instance, Wang *et al.* (2021) assessed drought characteristics at a global scale based on multiple indicators from 11 CMIP6 models. They discovered that, in the 21st century, numerous regions worldwide are anticipated to witness heightened frequencies, prolonged durations and expanded spatial coverage of droughts. Previous studies show that the Southeast Asian region

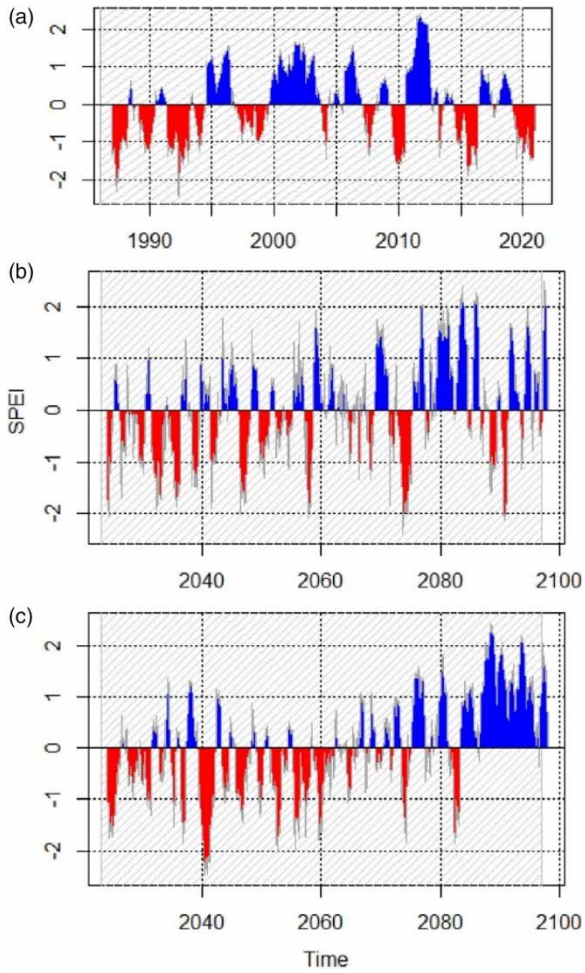


**Figure 7** | The evolution of the SPEI for 12-month timescale over the upper NRB during (a) observed period, and future periods (b) SSP2-4.5 and (c) SSP5-8.5, showing the variation in the duration, severity and intensity of dry and wet events.

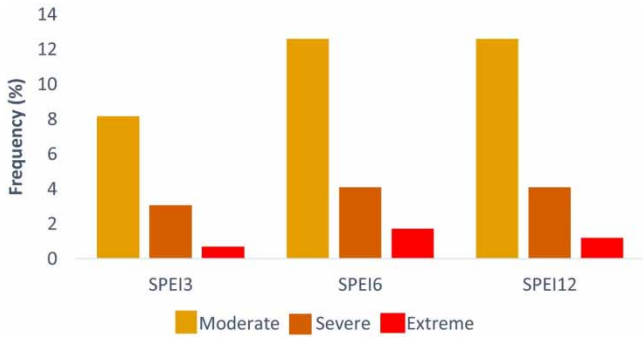


**Figure 8** | Observed frequencies of moderate, severe and extreme drought at SPEI3, SPEI6 and SPEI12 timescales over the upper NRB.

would experience more droughts under the scenarios SSP1-2.6, SSP2-4.5 and SSP5-8.5 (Byakatonda *et al.* 2021; Zeng *et al.* 2022).

This region, particularly Thailand and the Mekong River Basin, is also projected to have a similar temporal drought pattern when using different indices at different timescales (Thilakarathne & Sridhar 2017; Muangthong *et al.* 2020; Khadka *et al.*

**Table 6** | Maximum and minimum duration, severity and intensity of SPEI3, SPEI6 and SPEI12 over the upper NRB (1986–2020)

| SPEI | Maximum (minimum) duration months | Maximum (minimum) severity | Maximum (minimum) intensity |
|---|---|---|---|
| SPEI3 | 5 (1) | −8.58 ( − 1.03) | −1.93 ( − 1.03) |
| SPEI6 | 9 (1) | −11.25 ( − 1.03) | −1.81 ( − 1.03) |
| SPEI12 | 12 (1) | −17.24 ( − 1.04) | −1.69 ( − 1.04) |

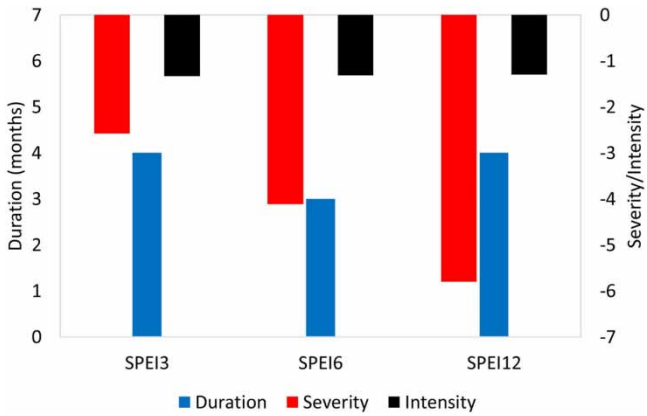


**Figure 9** | Average duration, severity and intensity of SPEI3, SPEI6 and SPEI12 over the upper NRB (1986–2020).

**Table 7** | Meteorological drought occurred in the dry season and wet season in upper NRB in the future under SSP2-4.5 and SSP5-8.5 scenarios

| | | Scenario | | | | |
|---|---|---|---|---|---|---|
| | | | SSP2-4.5 | | SSP5-8.5 | |
| Drought type | Season | Observed historical (1986–2020) | Near future (2023–2057) | Far future (2063–2097) | Near future (2023–2057) | Far future (2063–2097) |
| Mild and above (SPEI ≦ − 0.5) | Dry | 49% | 49% | 49% | 53% | 51% |
| | Wet | 51% | 51% | 51% | 47% | 49% |
| Severe and exceptional (SPEI ≦ − 1.3) | Dry | 51% | 49% | 53% | 48% | 46% |
| | Wet | 49% | 51% | 47% | 52% | 54% |

*Note*: Here the thresholds of drought are the same as that used by US Drought Monitor (Svoboda *et al.* 2002).

**Table 8** | Importance of variables for different climate change scenarios

| | Variable importance | | | | |
|---|---|---|---|---|---|
| Variables | Observed | SSP2-4.5 NF | SSP2-4.5 FF | SSP5-8.5 NF | SSP5-8.5 FF |
| Elevation | 52.1 | 50.2 | 51.4 | 49.4 | 53.4 |
| Slope | 17.2 | 13.2 | 13.4 | 17.1 | 21.2 |
| Intensity | 6.7 | 17.2 | 19.7 | 13.7 | 4.2 |
| Severity | 10.6 | 3.4 | 6.2 | 15.4 | 14.2 |
| Curvature | 5 | 3.2 | 3.3 | 2.6 | 2.6 |
| Duration | 4.5 | 11.6 | 2.2 | 1.4 | 2.3 |
| Aspect | 3.2 | 1.3 | 1.6 | 2.0 | 2.1 |

**Table 9** | Percentage area of different suitability classes under climate change scenarios

| Scenario | Time | Unsuitable | Marginally suitable | Moderately suitable | Highly suitable |
|---|---|---|---|---|---|
| Observed | | 0.1 | 28.5 | 42.2 | 29.2 |
| SSP2-4.5 | Near future | 0.1 | 27.9 | 45.2 | 26.8 |
| SSP2-4.5 | Far future | 0.2 | 28.0 | 44.8 | 27.0 |
| SSP5-8.5 | Near future | 0.2 | 23.0 | 48.4 | 28.5 |
| SSP5-8.5 | Far future | 0.1 | 22.0 | 46.2 | 31.7 |

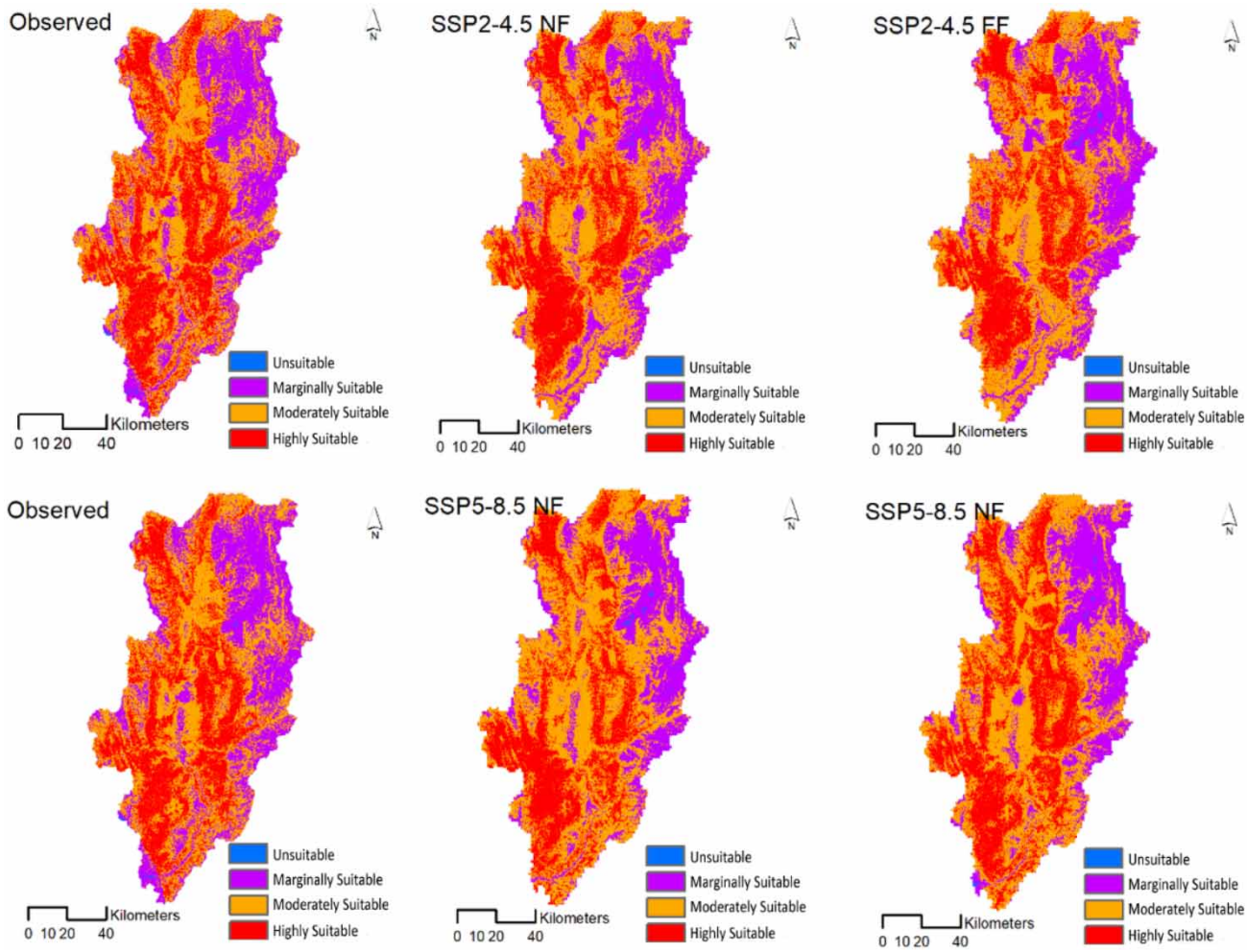


**Figure 10** | Maize suitability area projected using observed and projected climate change scenarios based on the maximum entropy model.

2021). Our analyses of drought characteristics over the upper NRB based on the 3-, 6- and 12-month SPEI for the period beginning 1986–2020 showed longer droughts in the upper region of the basin, which is more intense in terms of water demands for agriculture due to lack of irrigation facilities (Chaowiwat *et al.* 2016). It is now accepted that climate change has altered the patterns of rainfall, resulting in more frequent extreme weather events such as drought and flood (Tabari 2020). Our results of spatial and temporal evolution of dry and wet events captured by 3-, 6- and 12-month timescales of SPEI would have crucial implications on agriculture and community resilience. It is shown that dry conditions were

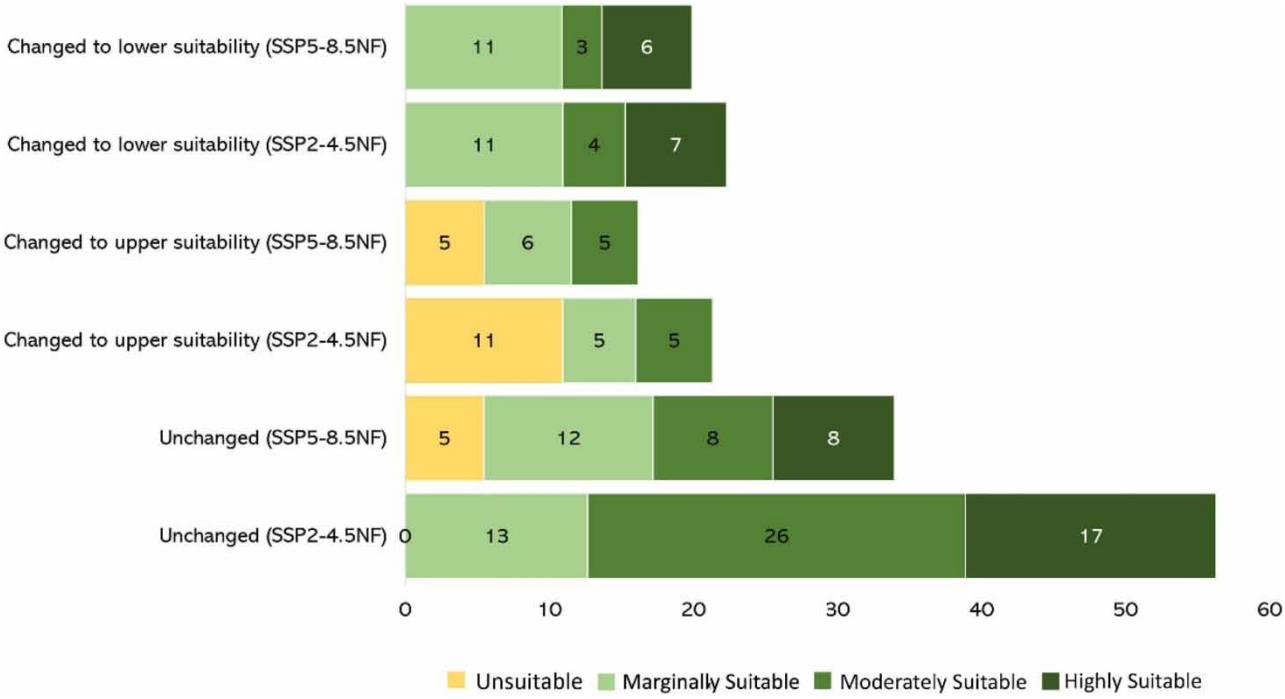


**Figure 11** | Change in maize production suitability areas under climate change scenarios (SSP2-4.5 and SSP5-8.5) in the near future.

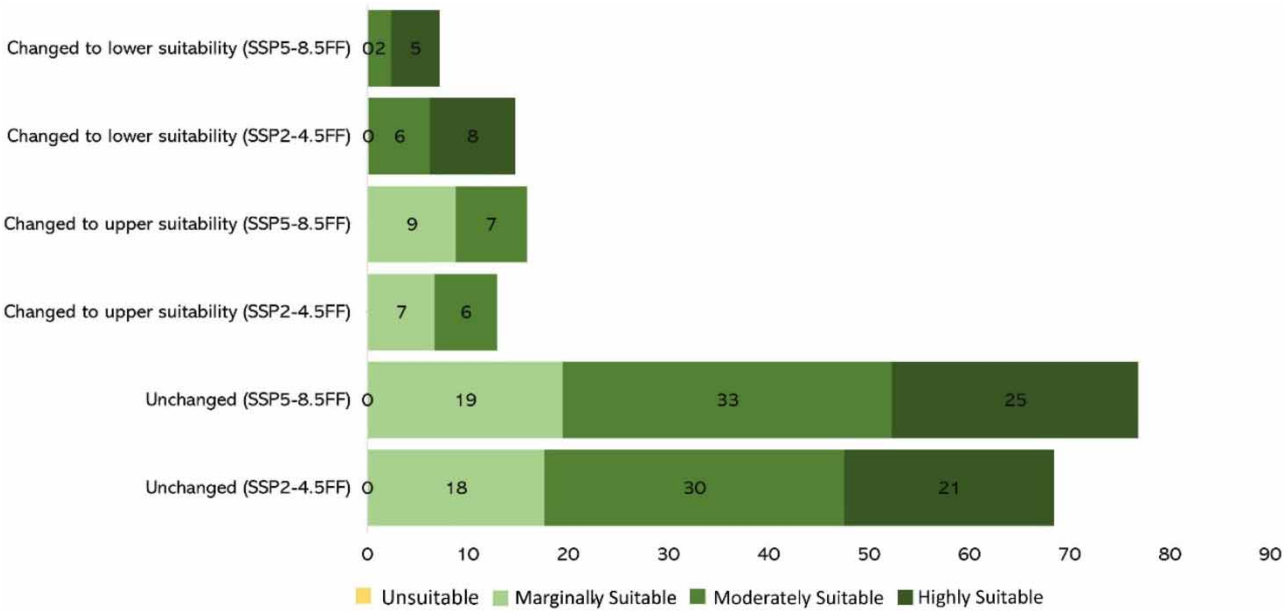


**Figure 12** | Change in maize production suitability areas under climate change scenarios (SSP2-4.5 and SSP5-8.5) in the far future.

predominant during the observed period than in the future. The seasonal drought is similar for wet and dry seasons while the FF period seems to experience wetter conditions, particularly under SSP5-8.5 scenario. The pattern of the temporal evolution of dry/wet events in the basin can be due to the influence of the high variability of seasonal and annual rainfall in the Southeast Asia region. The severe drought in 2016 along Southeast Asia is believed to be strongly linked to the super El Niño (Li *et al.* 2022). This study also captured the worst drought events during the 2015–2016 (Zenkoji *et al.* 2019) and 2019–2020 periods (NASA 2020) in Thailand.

### 4.2. Seasonal drought impact

The agriculture sector is vulnerable to climate, and it is especially important to identify the most appropriate tools for monitoring the impact of the weather on crops, and particularly the impact of drought. Drought indices calculated at different timescales (SPI or SPEI) are most closely correlated with crop yield, suggesting different patterns of yield response to drought depending on the region (Peña-Gallardo *et al.* 2019). As a paddy crop, the impact of rice yield is related to precipitation, as illustrated by previous studies (Thuy & Anh 2015; Chen *et al.* 2020). According to Kang *et al.* (2021), the increase in precipitation and $CO_2$ concentration in the Lower Mekong Basin could result in increased rice production. This study shows that drought conditions in both seasons are similar during the observed period. In the FF period under SSP2-4.5, the occurrence of dry season drought is elevated. Conversely, under SSP5-8.5, there is a higher prevalence of mild drought during the dry season, along with increased occurrences of severe and exceptional drought during the wet seasons. Considering the uneven distribution of irrigation facilities, and spatial and seasonal heterogeneity in future drought projections (Prabnakorn *et al.* 2018), further studies are needed to investigate how future changes in drought influence water security and crop production in the upper NRB and explore possible adaptation strategies.

### 4.3. Potential implication for maize cultivation area

Our study offers valuable insights into the present and projected suitability of maize in the upper NRB under two climate scenarios. The findings demonstrate a redistribution of maize-suitable areas in response to climate change, particularly under drought projections for both NF and FF scenarios. Regarding drought, the current findings align with the work of Rangwala & Miller (2012), who emphasized the importance of drought severity in crop distribution models. In addition, a study by Diffenbaugh *et al.* (2018) demonstrated the influence of drought intensity on crop suitability, which is consistent with the results showing the relevance of intensity in the SSP2-4.5 scenario. Looking into future scenarios, the projection of increased unsuitable areas is consistent with the predictions of Chen *et al.* (2020), who forecasted worsening agricultural conditions due to climate change. Regarding land-use changes, the results corroborate with the studies of Ty *et al.* (2022), which found shifts in land-use classes under different climate scenarios, supporting the notion that land-use changes are scenario dependent.

## 5. CONCLUSION

Based on the observed climate data and an average of four CMIP6 models under two climate change scenarios, this study examines the observed and future drought characteristics using SPEI in the upper NRB. This study highlights the contrasting changes in observed and future periods, and in the dry and wet seasons. The conclusions are as follows.

(1) There is an increasing trend of SPEI in the whole year and wet season of future period under SSP2-4.5 and SSP5-8.5 scenarios, but no significant and decreasing trend during the observed period for all seasons. The future trend in dry season drought is higher than the wet season. The wet season will be wetter in the future compared to the observed period, particularly during the FF under SSP5-8.5 scenario.
(2) Based on SPEI, the upper region of the basin experienced extended and severe drought, while the intensity of drought was higher in the lower region during the observed period. Moreover, in the NF, both scenarios show longer drought in the upper region, while the FF under SSP2-4.5 shows a longer drought in the mid-region and SSP5-8.5 shows a longer drought along the lower stretch of the basin.
(3) The results indicate that the moderate drought was higher than the severe and extreme droughts during the observed period over the upper NRB. The longest short-term drought (SPEI3) was observed in 2019/2020 with a duration of 5 months and a total severity of −8.58. Moreover, the longest duration of 9 and 12 months were observed for SPEI6 and SPEI12, respectively.
(4) The study findings provide valuable insights into the topographical factors influencing maize cultivation areas in the upper NRB and offer valuable implications for agricultural planning and climate change adaptation in the region. Moreover, the results indicate a redistribution of maize suitability areas under two climate change scenarios.

Since future droughts during the dry season are expected to become more severe while the wet season becomes wetter in the upper NRB, further studies are needed to investigate the application of differentiated adaptation strategies for different districts under drought conditions to increase maize production, particularly during the dry seasons, in the face of a changing climate.

## ACKNOWLEDGEMENTS

The authors would like to acknowledge the Thai Meteorological Department (TMD), Royal Irrigation Department (RID) and Office Agricultural Economics (OAE) of Thailand for providing data for this study. We are grateful for the invaluable insights and constructive feedback provided by the anonymous reviewers, whose expertise has truly enhanced the quality of our work.

## DATA AVAILABILITY STATEMENT

Data cannot be made publicly available; readers should contact the corresponding author for details.

## CONFLICT OF INTEREST

The authors declare there is no conflict.

## REFERENCES

Aguirre-Gutiérrez, J., Carvalheiro, L. G., Polce, C., van Loon, E. E., Raes, N., Reemer, M. & Biesmeijer, J. C. 2013 Fit-for-purpose: species distribution model performance depends on evaluation criteria–Dutch hoverflies as a case study. *PLoS one* **8** (5), e63708.

Ahmadalipour, A., Moradkhani, H. & Svoboda, M. 2017 Centennial drought outlook over the CONUS using NASA-NEX downscaled climate ensemble. *International Journal of Climatology* **37** (5), 2477–2491. doi:10.1002/joc.4859.

Allen, R. G., Pereira, L. S., Raes, D. & Smith, M. 1998 *FAO Irrigation and Drainage Paper No. 56 - Crop Evapotranspiration*.

Amnuaylojaroen, T., Chanvichit, P., Janta, R. & Surapipith, V. 2021 Projection of rice and maize productions in northern Thailand under climate change scenario RCP8.5. *Agriculture (Switzerland)* **11** (1), 1–15. doi:10.3390/agriculture11010023.

Arunrat, N., Sereenonchai, S., Chaowiwat, W. & Wang, C. 2022 Climate change impact on major crop yield and water footprint under CMIP6 climate projections in repeated drought and flood areas in Thailand. *Science of the Total Environment* **807**, 150741. Elsevier B.V. doi:10.1016/j.scitotenv.2021.150741.

Ashraf, M. & Routray, J. K. 2015 Spatio-temporal characteristics of precipitation and drought in Balochistan Province, Pakistan. *Natural Hazards*, **77**, 229–254.

Baicha, W. 2016 Land use dynamics and land cover structure change in Thailand (as exemplified by mountainous Nan Province. *Geography and Natural Resources* **37** (1), 87–92. doi:10.1134/S1875372816010121.

Brown, M. E., Antle, J. M., Backlund, P., Carr, E. R., Easterling, W. E., Walsh, M. K., Ammann, C., Attavanich, W., Barrett, C. B., Bellemare, M. F., Dancheck, V., Funk, C., Grace, K., Ingram, J. S. I., Jiang, H., Maletta, H., Mata, T., Murray, A., Ngugi, M., Ojima, D., O'Neill, B. & Tebaldi, C. 2015 *Climate change, global food security and the US food system.* MPRA Paper No. 105772. Available online at https://mpra.ub.uni-muenchen.de/105772/ (Accessed in April 2023).

Byakatonda, J., Parida, B. P., Moalafhi, D. B. & Kenabatho, P. K. 2018 Analysis of long term drought severity characteristics and trends across semiarid Botswana using two drought indices. *Atmospheric research* **213**, 492–508. doi:10.1016/j.atmosres.2018.07.002.

Chaowiwat, W., Boonya-aroonnet, S. & Weesakul, S. 2016 Impact of climate change assessment on agriculture water demand in Thailand. *Naresuan University Engineering Journal* **1**, 35–42.

Chen, X., Wang, L., Niu, Z., Zhang, M., Li, J. & Chen, X. 2020 The effects of projected climate change and extreme climate on maize and rice in the Yangtze River Basin, China. *Agricultural and Forest Meteorology* **282–283**, 107867. Elsevier. doi:10.1016/j.agrformet.2019.107867.

Chuenchum, P., Suttinon, P. & Ruangrassamee, P. 2017 *Input-Output Analysis of Water Deficits in Nan River Basin, Thailand*. In: THA 2017 International Conference on Water Management and Climate Change Towards Asia's Water-Energy-Food Nexus, Bangkok (pp. 265–271).

Cook, B. I., Mankin, J. S., Marvel, K., Williams, A. P., Smerdon, J. E. & Anchukaitis, K. J. 2020 Twenty-First century drought projections in the CMIP6 forcing scenarios. *Earth's Future* **8** (6), 1–20. doi:10.1029/2019EF001461.

Dai, M., Huang, S., Huang, Q., Leng, G., Guo, Y., Wang, L., Fang, W., Li, P. & Zheng, X. 2020 Assessing agricultural drought risk and its dynamic evolution characteristics. *Agricultural Water Management* **231**, 106003. Elsevier. doi:10.1016/j.agwat.2020.106003.

Diffenbaugh, N. S., Singh, D. & Mankin, J. S. 2018 Unprecedented climate events: Historical changes, aspirational targets, and national commitments. *Science Advances* **4** (2), 1–10. doi:10.1126/sciadv.aao3354.

Döscher, R., Acosta, M., Alessandri, A., Anthoni, P., Arneth, A., Arsouze, T., Bergmann, T., Bernadello, R., Bousetta, S., Caron, L. P. & Carver, G. 2021 The EC-earth3 Earth system model for the climate model intercomparison project 6. *Geoscientific Model Development Discussions* **2021**, 1–90.

Dunne, J. P., Horowitz, L. W., Adcroft, A. J., Ginoux, P., Held, I. M., John, J. G., Krasting, J. P., Malyshev, S., Naik, V., Paulot, F. & Shevliakova, E. 2020 The GFDL Earth System Model version 4.1 (GFDL-ESM 4.1): Overall coupled model description and simulation characteristics. *Journal of Advances in Modeling Earth Systems* **12**(11), e2019MS002015.

Eyring, V., Cox, P. M., Flato, G. M., Gleckler, P. J., Abramowitz, G., Caldwell, P., Collins, W. D., Gier, B. K., Hall, A. D., Hoffman, F. M. & Hurtt, G.C. 2019 Taking climate model evaluation to the next level. *Nature Climate Change* **9** (2), 102–110. doi:10.1038/s41558-018-0355-y.

Fang, J. & Su, Y. 2019 Effects of soils and irrigation volume on maize yield, irrigation water productivity, and nitrogen uptake. *Scientific Reports* **9** (1), 1–11. doi:10.1038/s41598-019-41447-z.

Feng, Y., Cui, N., Zhao, L., Gong, D. & Zhang, K. 2017 Spatiotemporal variation of reference evapotranspiration during 1954–2013 in Southwest China. *Quaternary International*, **441**, 129–139.

Fu, Z., Li, Z., Cai, C., Shi, Z., Xu, Q. & Wang, X. 2011 Soil thickness effect on hydrological and erosion characteristics under sloping lands: A hydropedological perspective. *Geoderma* **167–168**, 41–53. Elsevier B.V. doi:10.1016/j.geoderma.2011.08.013.

Fluixá-Sanmartín, J., Foehn, A., Travaglini, E., Alesina, S., Montero-Rubert, R. & García Hernández, J. 2016 *TeREsA – Technical Manual v1.1*. CREALP Group, Switzerland.

Gentle, P. & Maraseni, T. N. 2012 Climate change, poverty and livelihoods: Adaptation practices by rural mountain communities in Nepal. *Environmental Science and Policy* **21**, 24–34. Elsevier Ltd. doi:10.1016/j.envsci.2012.03.007.

Gornall, J., Betts, R., Burke, E., Clark, R., Camp, J., Willett, K. & Wiltshire, A. 2010 Implications of climate change for agricultural productivity in the early twenty-first century. *Philosophical Transactions of the Royal Society B: Biological Sciences* **365** (1554), 2973–2989. doi:10.1098/rstb.2010.0158.

Grudloyma, P. 2014 Country report Maize in Thailand. In *12th Asian Maize Conference and Expert Consultation on Maize for Food, Feed, Nutrition and Environmental Security*. pp. 326–331.

Guisan, A. & Zimmermann, N. E. 2000 Predictive habitat distribution models in ecology. *Ecological modelling* **135** (2–3), 147–186.

Hargreaves, G. H. & Samani, Z. A. 1985 Reference crop evapotranspiration from temperature. *Applied engineering in agriculture*, **1**(2), 96-99.

He, Q. J. & Zhou, G. S. 2012 The climatic suitability for maize cultivation in China. *Chinese Science Bulletin* **57** (4), 395–403. doi:10.1007/s11434-011-4807-2.

He, Q. & Zhou, G. 2016 Climate-associated distribution of summer maize in China from 1961 to 2010. *Agriculture, Ecosystems and Environment* **232**, 326–335. Elsevier B.V. doi:10.1016/j.agee.2016.08.020.

Heim, R. R. 2002 A review of twentieth-century drought indices used in the United States. *Bulletin of the American Meteorological Society*, **83** (8), 1149–1166.

Hernandez, P. A., Graham, C. H., Master, L. L. & Albert, D. L. 2006 The effect of sample size and species characteristics on performance of different species distribution modeling methods. *Ecography*, 29(5), 773-785.

Iqbal, Z., Shahid, S., Ahmed, K., Ismail, T., Ziarh, G. F., Chung, E. S. & Wang, X. 2021 Evaluation of CMIP6 GCM rainfall in mainland Southeast Asia. *Atmospheric Research* **254**, 105525. Elsevier B.V. doi:10.1016/j.atmosres.2021.105525.

Jiang, T., Su, X., Singh, V. P. & Zhang, G. 2022 Spatio-temporal pattern of ecological droughts and their impacts on health of vegetation in northwestern China. *Journal of Environmental Management* **305**, 114356. Elsevier Ltd. doi:10.1016/j.jenvman.2021.114356.

Kang, H., Sridhar, V., Mainuddin, M. & Trung, L. D. 2021 Future rice farming threatened by drought in the Lower Mekong Basin. *Scientific Reports* **11** (1), 1–15. Nature Publishing Group UK. doi:10.1038/s41598-021-88405-2.

Kendall, M. G. 1975 *Rank Correlation Methods*. London, UK, Charles Griffin.

Khadka, D., Babel, M. S., Shrestha, S., Virdis, S. G. & Collins, M. 2021 Multivariate and multi-temporal analysis of meteorological drought in the northeast of Thailand. *Weather and Climate Extremes* **34**, 100399. Elsevier B.V. doi:10.1016/j.wace.2021.100399.

Kogo, B. K., Kumar, L., Koech, R. & Kariyawasam, C. S. 2019 Modelling climate suitability for rainfed maize cultivation in Kenya using a maximum entropy (MAXENT) approach. *Agronomy* **9** (11). doi:10.3390/agronomy9110727.

Lee, S. H., Yoo, S. H., Choi, J. Y. & Bae, S. 2017 Assessment of the impact of climate change on drought characteristics in the Hwanghae Plain, North Korea using time series SPI and SPEI: 1981–2100. Water *(Switzerland) 9(8)*. https://doi.org/10.3390/w9080579.

Li, S. Y., Miao, L. J., Jiang, Z. H., Wang, G. J., Gnyawali, K. R., Zhang, J., Zhang, H., Fang, K., He, Y. & Li, C. 2020 Projected drought conditions in Northwest China with CMIP6 models under combined SSPs and RCPs for 2015–2099. *Advances in Climate Change Research* **11** (3), 210–217. doi:10.1016/j.accre.2020.09.003.

Li, Y., Lu, H., Entekhabi, D., Gianotti, D. J. S., Yang, K., Luo, C., Feldman, A.F., Wang, W. & Jiang, R. 2022 Satellite-based assessment of meteorological and agricultural drought in Mainland Southeast Asia. *IEEE Journal of Selected Topics in Applied Earth Observations and Remote Sensing* **15**, 6180–6189. doi:10.1109/JSTARS.2022.3190438.

Liu, Y., Wang, Q., Yao, X., Jiang, Q., Yu, J. & Jiang, W. 2020 Variation in reference evapotranspiration over the Tibetan Plateau during 1961–2017: Spatiotemporal variations, future trends and links to other climatic factors. Water, *12(11), 3178*.

Lovato, T., Peano, D., Butenschön, M., Materia, S., Iovino, D., Scoccimarro, E., Fogli, P.G., Cherchi, A., Bellucci, A., Gualdi, S. & Masina, S. 2022 CMIP6 simulations with the CMCC Earth System Model (CMCC-ESM2). *Journal of Advances in Modeling Earth Systems* **14** (3). doi:10.1029/2021MS002814.

Mann, H. B. 1945 Nonparametric tests against trend. Econometrica: Journal of the Econometric Society, *245-259*.

Manning, M. R. 2006 The treatment of uncertainties in the fourth IPCC assessment report. Adv. Clim. Chang. Res. **2** (2006), 13–21.

Massonnet, F., Ménégoz, M., Acosta, M., Yepes-Arbós, X., Exarchou, E. & Doblas-Reyes, F. J. 2020 Replicability of the EC-Earth3 Earth system model under a change in computing environment. *Geoscientific Model Development* **13**(3), 1165-1178.

Ma, Q., Zhang, J., Sun, C., Guo, E., Zhang, F. & Wang, M. 2017 Changes of reference evapotranspiration and its relationship to dry/wet conditions based on the aridity index in the Songnen Grassland, northeast China. *Water* **9** (5), 316.

Mishra, A. K. & Singh, V. P. 2010 A review of drought concepts. *Journal of Hydrology* **391** (1–2), 202–216. Elsevier B.V. doi:10.1016/j.jhydrol.2010.07.012.

Muangthong, S., Chaowiwat, W., Sarinnapakorn, K. & Chaibandit, K. 2020 Prediction of future drought in Thailand under changing climate by using SPI and SPEI indices. *Mahasarakham International Journal of Engineering Technology* **6** (2), 48–56.

Muthuvel, D., Sivakumar, B. & Mahesha, A. 2023 Future global concurrent droughts and their effects on maize yield. *Science of the Total Environment* **855**, 158860. Elsevier B.V. doi:10.1016/j.scitotenv.2022.158860.

NASA. 2020 *Drought Hits Thailand*. Available from: https://earthobservatory.nasa.gov/images/146293/drought-hits-thailand.

Neswati, R., Baja, S. & Lopulisa, C. 2021 A modification of land suitability requirements for maize in the humid tropics of South Sulawesi. *IOP Conference Series: Earth and Environmental Science* **921** (1). doi:10.1088/1755-1315/921/1/012012.

Office of Agricultural Economics 2015 *Indicator of Agricultural Economics of Thailand 2014*. Office of Agricultural Economics, Thailand.

Office of Agricultural Economics 2017 *Agricultural Statistics of Thailand 2016*. Office of Agricultural Economics, Ministry of Agricultural and Cooperative in Thailand.

Office of the National Economic and Social Development Board 2017 *Annual population birth and mortality throughout the Kingdom 1993–2016*. Office of the National Economic and Social Development Board, Thailand.

Peña-Gallardo, M., Vicente-Serrano, S. M., Domínguez-Castro, F. & Beguería, S. 2019 The impact of drought on the productivity of two rainfed crops in Spain. *Natural Hazards and Earth System Sciences* **19** (6), 1215–1234. doi:10.5194/nhess-19-1215-2019.

Petpongpan, C. E. C., Ekkawatpanit, C., Visessri, S. & Kositgittiwong, D. 2021 Projection of hydro-climatic extreme events under climate change in Yom and Nan River Basins, Thailand. *Water* **13** (5), 665.

Prabnakorn, S., Maskey, S., Suryadi, F. X. & de Fraiture, C. 2018 Rice yield in response to climate trends and drought index in the Mun River Basin, Thailand. *Science of the Total Environment* **621**, 108–119. Elsevier B.V. doi:10.1016/j.scitotenv.2017.11.136.

Phillips, S. J., Anderson, R. P. & Schapire, R. E. 2006 Maximum entropy modeling of species geographic distributions. *Ecological modelling* **190** (3–4), 231–259.

Rangwala, I. & Miller, J. R. 2012 Climate change in mountains: A review of elevation-dependent warming and its possible causes. *Climatic Change* **114** (3–4), 527–547. doi:10.1007/s10584-012-0419-3.

Riahi, K., Rao, S., Krey, V., Cho, C., Chirkov, V., Fischer, G., Kindermann, G., Nakicenovic, N. & Rafaj, P. 2011 RCP 8.5-A scenario of comparatively high greenhouse gas emissions. *Climatic Change* **109** (1), 33–57. doi:10.1007/s10584-011-0149-y.

Schwarzwald, K., Poppick, A., Rugenstein, M., Bloch-Johnson, J., Wang, J., McInerney, D. & Moyer, E. J. 2021 Changes in future precipitation mean and variability across scales. *Journal of Climate* **34** (7), 2741–2758. Center for Robust Decision-Making on Climate and Energy Policy, The University of Chicago, Chicago, IL, United States. doi:10.1175/JCLI-D-20-0001.1.

Sen, P. K. 1968 Estimates of the regression coefficient based on Kendall's tau. *Journal of the American statistical association*, 1379-1389.

Shrestha, R. & Arunyawat, S. 2017 Adaptation to climate change by rural ethnic communities of Northern Thailand. doi:10.3390/cli5030057.

Shrestha, S., Chapagain, R. & Babel, M. S. 2017 Quantifying the impact of climate change on crop yield and water footprint of rice in the Nam Oon Irrigation Project, Thailand. *Science of the Total Environment* **599–600**, 689–699. Elsevier B.V. doi:10.1016/j.scitotenv.2017.05.028.

Supharatid, S., Nafung, J. & Aribarg, T. 2021 Projected changes in temperature and precipitation over mainland Southeast Asia by CMIP6 models. *Journal of Water and Climate Change*, 1–20. doi:10.2166/wcc.2021.015.

Svoboda, M., LeComte, D., Hayes, M., Heim, R., Gleason, K., Angel, J., Rippey, B., Tinker, R., Palecki, M., Stooksbury, D. & Miskus, D. 2002 The drought monitor. *Bulletin of the American Meteorological Society*, **83**(8), 1181–1190.

Swart, N. C., Cole, J. N., Kharin, V. V., Lazare, M., Scinocca, J. F., Gillett, N. P., Anstey, J., Arora, V., Christian, J. R., Hanna, S. & Jiao, Y. 2019 The Canadian Earth System Model version 5 (CanESM5.0.3). *Geoscientific Model Development Discussions* **5**, 1–68. doi:10.5194/gmd-2019-177.

Tabari, H. 2020 Climate change impact on flood and extreme precipitation increases with water availability. *Scientific Reports* **10** (1), 1–10. Nature Publishing Group UK. doi:10.1038/s41598-020-70816-2.

Tashayo, B., Honarbakhsh, A., Akbari, M. & Eftekhari, M. 2020 Land suitability assessment for maize farming using a GIS-AHP method for a semi- arid region, Iran. *Journal of the Saudi Society of Agricultural Sciences* **19** (5), 332–338. King Saud University & Saudi Society of Agricultural Sciences. doi:10.1016/j.jssas.2020.03.003.

Themeßl, M. J., Gobiet, A. & Heinrich, G. 2012 Empirical-statistical downscaling and error correction of regional climate models and its impact on the climate change signal. *Climatic Change* **112** (2), 449–468. doi:10.1007/s10584-011-0224-4.

Thilakarathne, M. & Sridhar, V. 2017 Characterization of future drought conditions in the Lower Mekong River Basin. *Weather and Climate Extremes* **17**, 47–58. Elsevier Ltd. doi:10.1016/j.wace.2017.07.004.

Thuy, N. N. & Anh, H. H. 2015 'Vulnerability of rice production in Mekong river delta under impacts from floods, salinity and climate change. *International Journal on Advanced Science, Engineering and Information Technology* **5** (4), 272–279. doi:10.18517/ijaseit.5.4.545.

Ty, T. V., Lavane, K., Nguyen, P. C., Downes, N. K., Nam, N. D. G., Minh, H. V. T. & Kumar, P. 2022 Assessment of relationship between climate change, drought, and land use and land cover changes in a semi-Mountainous area of the Vietnamese Mekong delta. *Land* **11** (12). doi:10.3390/land11122175.

Ukkola, A. M., De Kauwe, M. G., Roderick, M. L., Abramowitz, G. & Pitman, A. J. 2020 Robust future changes in meteorological drought in CMIP6 projections despite uncertainty in precipitation. *Geophysical Research Letters* **47** (11), 0–3. doi:10.1029/2020GL087820.

Vicente-Serrano, S. M., Beguería, S. & López-Moreno, J. I. 2010 A multiscalar drought index sensitive to global warming: The standardized precipitation evapotranspiration index. *Journal of Climate* **23** (7), 1696–1718. doi:10.1175/2009JCLI2909.1.

Wang, T., Tu, X., Singh, V. P., Chen, X. & Lin, K. 2021 Global data assessment and analysis of drought characteristics based on CMIP6. *Journal of Hydrology* **596**, 126091. Elsevier B.V. doi:10.1016/j.jhydrol.2021.126091.

Wangpimool, W., Pongput, K., Sukvibool, C., Sombatpanit, S. & Gassman, P. W. 2013 The effect of reforestation on stream flow in Upper Nan river basin using Soil and Water Assessment Tool (SWAT) model. *International Soil and Water Conservation Research* **1** (2), 53–63. Elsevier Masson SAS. doi:10.1016/S2095-6339(15)30039-3.

World Meterological Organization (WMO) and Global Water Partnership (GWP). 2016 *Handbook of Drought Indicators and Indices*. Integrated. Edited by M. S. and B. A. Fuchs. WMO & GWP, Geneva, Switzerland. doi:10.1136/bmj.1.2366.1068-b.

World Meteorological Organization (WMO). 2012 *Standardized Precipitation Index User Guide* (M. Svoboda, M. Hayes and D. Wood). (World Meteorological Organization-No. 1090), Geneva

Yue, Y., Zhang, P. & Shang, Y. 2019 The potential global distribution and dynamics of wheat under multiple climate change scenarios. *Science of the Total Environment* **688** (19), 1308–1318. Elsevier B.V. doi:10.1016/j.scitotenv.2019.06.153.

Yue, Y., Yan, D., Yue, Q., Ji, G. & Wang, Z. 2021 Future changes in precipitation and temperature over the Yangtze River Basin in China based on CMIP6 GCMs. *Atmospheric Research* **264**, 105828. Elsevier B.V. doi:10.1016/j.atmosres.2021.105828.

Zeng, J., Li, J., Lu, X., Wei, Z., Shangguan, W., Zhang, S., Dai, Y. & Zhang, S. 2022 Assessment of global meteorological, hydrological and agricultural drought under future warming based on CMIP6. *Atmospheric and Oceanic Science Letters* **15** (1), 100143. Elsevier B.V. doi:10.1016/j.aosl.2021.100143.

Zenkoji, S., Tebakari, T. & Dotani, K. 2019 Rainfall and reservoirs situation under the worst drought recorded in the Upper Chao Phraya River Basin, Thailand. *Journal of Japan Society of Civil Engineers, Ser. G (Environmental Research)* **75** (5), I_115–I_124. doi:10.2208/jscejer.75.i_115.

Zhai, J., Mondal, S. K., Fischer, T., Wang, Y., Su, B., Huang, J., Tao, H., Wang, G., Ullah, W. & Uddin, M. J. 2020 Future drought characteristics through a multi-model ensemble from CMIP6 over South Asia. *Atmospheric Research* **246**, 105111. Elsevier. doi:10.1016/j.atmosres.2020.105111.

Zhu, Y. Y. & Yang, S. 2020 Evaluation of CMIP6 for historical temperature and precipitation over the Tibetan Plateau and its comparison with CMIP5. *Advances in Climate Change Research* **11** (3), 239–251. Elsevier Ltd. doi:10.1016/j.accre.2020.08.001.

First received 26 August 2023; accepted in revised form 14 December 2023. Available online 27 December 2023